

# UC Berkeley

## UC Berkeley Previously Published Works

### Title

Advances in supramolecular host-mediated reactivity

### Permalink

<https://escholarship.org/uc/item/02s7f40m>

### Journal

Nature Catalysis, 3(12)

### ISSN

2520-1158

### Authors

Morimoto, Mariko  
Bierschenk, Stephen M  
Xia, Kay T  
et al.

### Publication Date

2020-12-01

### DOI

10.1038/s41929-020-00528-3

Peer reviewed

# 1 **Advances in supramolecular host-mediated reactivity**

2 **Mariko Morimoto<sup>†</sup>, Stephen M. Bierschenk<sup>†</sup>, Kay T. Xia<sup>†</sup>, Robert G. Bergman, Kenneth N.**  
3 **Raymond, F. Dean Toste\*.**

4 Chemical Sciences Division, Lawrence Berkeley National Laboratory and Department of  
5 Chemistry, University of California, Berkeley, California 94720, United States

## 6 **Abstract**

7         Since the trailblazing discoveries of Lehn, Cram and Pedersen, supramolecular chemistry  
8 has established itself as a cornerstone of organic chemistry. Supramolecular hosts offer defined  
9 microenvironments that mimic the active sites of enzymes, utilizing specific host-guest  
10 interactions to enable remarkable rate enhancements and product selectivity. The development of  
11 a diverse array of self-assembled hosts, coupled with the increased demand for shorter and greener  
12 synthetic routes, have spurred significant progress in the field of supramolecular catalysis. This  
13 review covers recent advances in the field, ranging from novel organic reactivity aided by  
14 supramolecular hosts to catalytic cooperation between hosts and organometallic compounds or  
15 metal nanoparticles. Strides have also been made in the synthetic application of these hosts in site-  
16 selective substrate modifications and challenging photochemical reactions. These efforts have  
17 enabled the incorporation of non-covalent macromolecular catalysis in natural product syntheses,  
18 evidencing their unique advantages as a synthetic tool, and their powerful potential for practical  
19 applications.

## 20 **Introduction**

21         In nature, precise molecular reactivity is facilitated by a cascade of enzymes that  
22 collectively lower the activation barriers of complex, multi-step transformations under mild

23 conditions.<sup>1-3</sup> Synthetic chemists have long sought to attain such molecular precision, via tuning  
24 of reaction conditions including solvent, temperature, and catalyst design. One such approach was  
25 the development of supramolecular host molecules, whose reactivity bears clear resemblance to  
26 that of enzymatic catalysis.<sup>4-6</sup> Like enzymatic active sites, the defined microenvironments within  
27 these host molecules demonstrate selective guest binding and harness non-covalent interactions to  
28 induce reactivity and selectivity not observed in bulk solution.

29         In the decades following the initial discovery of crown ethers,<sup>7</sup> cryptands,<sup>8</sup> and  
30 carcerands,<sup>9,10</sup> the structural diversity of supramolecular hosts has undergone tremendous growth.  
31 Early covalent hosts including cyclodextrins and cucurbiturils remain instrumental to  
32 supramolecular catalysis, largely due to their commercial accessibility and amenability to large-  
33 scale synthesis.<sup>11-16</sup> A significant challenge for this class of hosts, however, is the formation of  
34 larger assemblies, which necessitates the synthesis of increasingly complex covalent scaffolds with  
35 each iteration. Multimeric resorcinarene hosts,<sup>17,18</sup> calixarene-based capsules,<sup>19</sup> and dimeric  
36 “softball” hosts by Rebek and co-workers,<sup>20</sup> present one solution in which higher order structures  
37 are formed through the self-assembly of multiple covalent components. Another developing class  
38 of hosts are metal coordination cages, featuring transition metal vertices and ligands that form the  
39 edges or faces of the polyhedral framework.<sup>21,22</sup> While generally less robust than their covalent  
40 counterparts, coordination cages offer significantly more tunability in terms of size and charge,  
41 derived from variable ligand designs and metal oxidation states. This structural diversity of  
42 supramolecular hosts has spurred their utilization in a broad range of synthetic applications,  
43 ranging from homogeneous organic reactions to nanoparticle catalysis.

44         Supramolecular hosts provide an accessible means for synthetic chemists to exploit non-  
45 covalent macromolecular reactivity, particularly in non-biological processes. Remarkable

46 reactivity has been observed within these assemblies, with some catalysts attaining rate  
47 accelerations of a million-fold or more. The ability of these hosts to stabilize reactive  
48 intermediates, transition states, and excited states has enabled a growing number of challenging  
49 transformations to proceed under unconventionally mild conditions. Additionally, guest  
50 recognition and constrictive binding have promoted size-, site-, regio-, and enantioselective  
51 catalysis, epitomized by host-mediated asymmetric photochemical reactions and late-stage  
52 functionalization of natural products. While other synthetic catalysts require complex ligand  
53 scaffolds and careful control of reaction conditions to render selectivity, supramolecular catalysts  
54 readily self-assemble from simple components, providing a tailored microenvironment even under  
55 otherwise unfavourable reaction conditions. These exceptional properties and performance of  
56 supramolecular catalysts make them worthy targets for synthesis and warrant future studies into  
57 their application and mechanisms of action.

58         This review covers the major advancements made in the unique reactivity promoted by  
59 supramolecular hosts in the past five years.<sup>23-28</sup> We begin by highlighting new variations on well-  
60 established supramolecular organic reactivity, followed by organometallic reactions facilitated by  
61 supramolecular hosts. For the sake of brevity, this review only covers the reactivity of cages that  
62 assemble around or encapsulate the entirety of the transition metal catalyst. Sterically hindered or  
63 bifunctional ligands including highly functionalized N-heterocyclic carbenes and tethered peptide  
64 scaffolds have been shown to noncovalently influence transition metal reactivity, and are covered  
65 in other reviews.<sup>29-31</sup> Beyond simply enabling organic and organometallic reactivity,  
66 supramolecular hosts have also been shown to direct regio- and site-selectivity, representing an  
67 emerging, application-driven direction in the field. Other avenues of catalysis, including host-

68 mediated photochemical reactions, are also described, demonstrating the versatility of current  
69 state-of-the-art supramolecular catalysts.

## 70 **Organic Reactions Catalysed by Supramolecular Hosts**

71 Supramolecular catalysis is hallmarked by the ability of host molecules to stabilize  
72 encapsulated reactive species through a number of non-covalent interactions, thereby decreasing  
73 the free energy gap between reactant states and transition states. Drawing on multiple stabilizing  
74 factors, remarkable catalytic activity has been observed within supramolecular hosts, inviting  
75 comparisons to the activity of enzymes. Specifically, supramolecular Brønsted acid catalysis has  
76 been enabled via favourable Coulombic and cation- $\pi$  interactions within hosts, allowing (for  
77 example) Brønsted acid catalysis to take place under usually prohibitive basic, aqueous  
78 conditions.<sup>32</sup> This reactivity is demonstrated by an aza-Prins rearrangement, catalysed by the  
79 triscatecholate based dodecaanionic host-**1** which has been studied extensively by Raymond,  
80 Bergman, Toste, and co-workers. This host effectively stabilizes hydrolytically unstable cationic  
81 species, including iminium ions within its core, despite water as solvent,<sup>33</sup> which in the aza-Prins  
82 reaction enabled the intramolecular nucleophilic addition of a pendant alkene to an *in-situ*  
83 generated iminium ion (**Figure 1a**).<sup>34</sup> The encapsulated addition complex underwent an unusual  
84 1,5-hydride shift, facilitated by the constrictive nature of the interior of host-**1**. The product  
85 generated cannot be accessed under conventional acid catalysis in the absence of the host, and  
86 demonstrates the role that supramolecular catalysts can play in accessing atypical reaction  
87 pathways by an acid catalysed mechanism.

88 Accessing more complex transformations to yield diverse product scaffolds has remained  
89 an outstanding challenge in supramolecular chemistry. One solution to this issue takes advantage  
90 of the stability of iminium ion intermediates within **1** to access a multicomponent aza-Darzens

91 reaction via intermolecular nucleophilic addition.<sup>35</sup> This reaction, catalysed by host-1 (2-10  
92 mol%), provided *trans*-substituted aziridines as the major diastereomer. However, when host-1  
93 was blocked with a strongly binding guest, tetraethylammonium, the opposite *cis*-substituted  
94 diastereomer was observed as the major product in low conversions. In addition, typical acid  
95 catalysed aza-Darzens reactions provided *cis*-substituted aziridines, again highlighting the ability  
96 of supramolecular catalysis to access unusual reaction pathways.

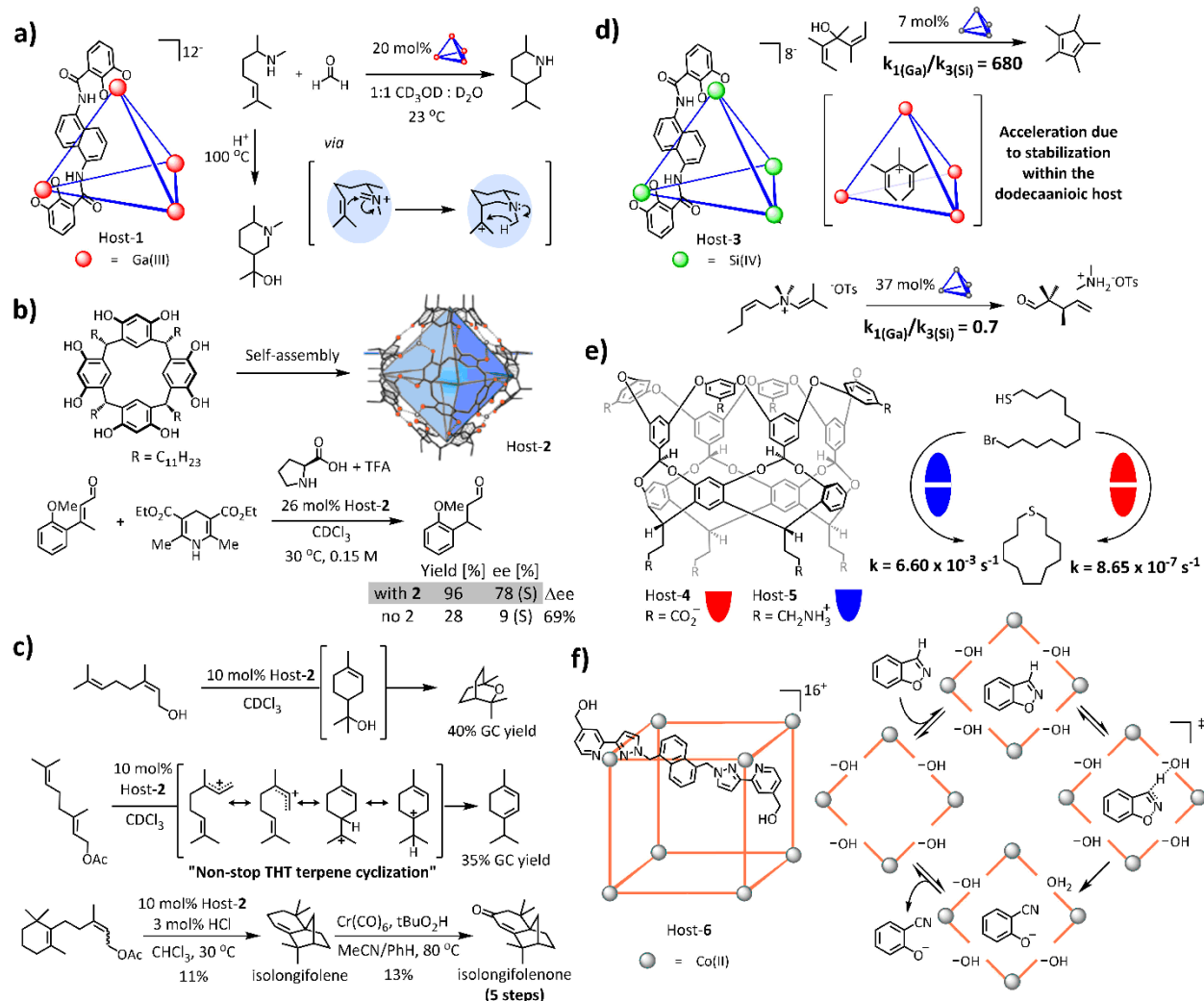
97         Supramolecular hosts also demonstrate the ability to modulate product selectivity in  
98 iminium catalysed reactions. Tiefenbacher and co-workers reported the selective 1,4-reduction of  
99  $\alpha,\beta$ -unsaturated cinnamaldehyde derivatives catalysed by chiral proline derivatives and  
100 resorcinarene host-2 (**Figure 1b**).<sup>36</sup> Host-2 self-assembles from six equivalents of resorcinarene in  
101 organic solvents, and is held together via phenolic hydrogen bonding. The phenolic units of **2** have  
102 a lower than expected pKa of 5.5-6 (rather than the typical pKa 10 for phenol) enabling them to  
103 function as a built-in source of acid. The polyaromatic nature of the ligands promote acid catalysis  
104 via stabilization of cationic intermediate due to favourable cation- $\pi$  interactions.<sup>17</sup> In Tiefenbacher  
105 and co-workers' report, a proline catalysed 1,4-reduction of  $\alpha,\beta$ -unsaturated aldehydes was  
106 subjected to hexamer **2**, and a significant change in the enantiomeric excess (ee) of the product  
107 aldehyde was measured. For an *ortho*-methoxy substituted cinnamaldehyde substrate, the **2**-  
108 catalyzed reaction yielded the corresponding product with 78% ee (S), compared to 9% ee (S) in  
109 the control reaction (69%  $\Delta$ ee). The change in the enantioselectivity of the reaction originates from  
110 host-2 blocking the less sterically hindered face of the aldehyde, generating a "mismatched" case  
111 with the proline derivatives. This causes the Hantzsch ester to deliver the hydride from the same  
112 face into which the proline chiral information projects.<sup>37</sup> Acid catalysis within host-2 was extended  
113 to a number of other transformations, such as the hydroxyalkylation reaction and cyclodehydration

114 reaction of alcohols with prenyl derivatives and the hydration of aryl alkynes.<sup>38-40</sup> Tiefenbacher  
115 and co-workers also disclosed an unusual carbonyl-olefin metathesis reaction within host-**2**  
116 enabled for the first time in the absence of strong Lewis Acids.<sup>41</sup> Addition of HCl as a cocatalyst  
117 in this system allowed reactions to proceed with 10 mol% host, in up to 98% yield, but with long  
118 reaction times (1-17d).

119 In an effort to extend supramolecular catalysis to more practical applications, Tiefenbacher  
120 and co-workers also investigated terpene cyclizations within host-**2**. Supramolecular terpene  
121 cyclization is an attractive, yet challenging target, as numerous products can be generated from a  
122 single terpene.<sup>42,43</sup> In their seminal report, nerol, geraniol and linalool were encapsulated and  
123 ionized within **2** to generate a variety of tail-to-head terpene (THT) cyclization products.<sup>44</sup> **2**-  
124 catalyzed nerol cyclization provided access to eucalyptol in useful yields (~40%), previously  
125 inaccessible via direct cyclization of nerol (**Figure 1c**). To probe leaving group effects, both  
126 geraniol and geranyl acetate were subjected to host-**2** catalysed conditions, and remarkably, both  
127 provided the same major product,  $\alpha$ -terpinene, suggesting that the initially formed transoid allylic  
128 carbocation directly isomerized to the cisoid allylic carbocation without the involvement of a  
129 linalyl intermediate. This result suggests that host-**2** facilitated a “non-stop” THT cyclization,  
130 where cationic intermediates undergo direct isomerization and addition reactions without  
131 interception by an external nucleophile, showcasing the ability of **2** to shield reactive  
132 intermediates.<sup>45</sup> Subsequent studies presented the concise synthesis of terpenoid natural products  
133 using THT cyclization, within host-**2**, to access the molecular skeleton of isolongifolenone,<sup>46</sup>  $\delta$ -  
134 Selinene,<sup>47</sup> and (-)-Presilphiperfolan-1 $\beta$ -ol (**Figure 1c**).<sup>48</sup> These represent the shortest total  
135 syntheses to date of these natural products, demonstrating the feasibility of supramolecular  
136 catalysts as powerful reagents in complex molecule synthesis.

137 In many cases the source of rate acceleration in supramolecular catalysis is poorly  
138 understood. To elucidate the effect of host charge, the Raymond, Bergman, and Toste groups  
139 reported a two-cage study on the rates of an acid-catalysed Nazarov cyclization.<sup>49</sup> The Nazarov  
140 cyclization, which proceeds with up to 10<sup>6</sup>-fold rate acceleration in the presence of dodecaanionic  
141 host-**1**, was subjected to the octaanionic Si<sup>IV</sup>-based host-**3** (**Figure 1d**). Host-**1** accelerated the rate  
142 680-fold more than host-**3**, due to its superior ability to stabilize the cationic intermediates and  
143 transition state of the Nazarov cyclization. For an overall charge-neutral Aza-Cope reaction  
144 catalysed by the constricted interior of the hosts, the rate should be independent of host charge  
145 because the single positive charge on the reactant does not change during the transformation—and  
146 indeed, the rates were found to be within error between hosts **1** and **3**. Despite being isostructural,  
147 hosts **1** and **3** exhibit contrasting reactivity due to their difference in charge. In a related study,  
148 Gibb and co-workers investigated the effect of charge on the macrocyclization of  $\alpha, \omega$  thioalkane  
149 halides in organic supramolecular capsules.<sup>50</sup> Two related capsules were synthesized: capsule **4**,  
150 containing pendant carboxylate anions, and capsule **5**, containing pendant ammonium cations  
151 (**Figure 1e**), which both self-assemble in solution to form homodimers that encapsulate  
152 hydrophobic molecules. Homodimer **5** catalysed the macrocyclization reaction to completion in a  
153 matter of minutes, while in the presence of the anionic homodimer **4**, the reaction required several  
154 weeks. This discrepancy in rate originates from stabilization of the thiolate anion (the active  
155 nucleophile), by cationic host **5**. These two studies emphasize the importance of charge and  
156 electrostatic fields in enabling catalytic pathways within supramolecular hosts.





157

## 158 Figure 1: Organic transformations catalysed by supramolecular hosts

159 **a)** Comparison of the aza-Prins reaction catalysed by host-1 and the formic acid catalysed  
 160 cyclization. **b)** Top: Self-Assembled resorcinarene host-2. Bottom: The asymmetric 1,4-reduction  
 161 of aldehydes facilitated by host 2. **c)** Top: nerol cyclization to give eucalyptol as the primary  
 162 product in the presence of host-2. Middle: the non-stop THT cyclization of geranyl acetate  
 163 catalysed by 2. Bottom: Terpene cyclization reaction in host-2 for the concise synthesis of  
 164 isolongifolenone. **d)** Charge study between host-3 (8<sup>-</sup> overall charge) and host-1 (12<sup>-</sup>  
 165 overall charge). Top: Nazarov cyclization. Bottom: Aza-Cope. **e)** Charge study on the macrocyclization  
 166 of thiols in the presence of polyanionic host-4 and polycationic host-5. **f)** Left: Cubic Co<sup>II</sup> based  
 167 supramolecular host-6. Right: catalytic cycle for the host-6 catalysed Kemp elimination.

168 In contrast to acid catalysis, Ward and co-workers have investigated base catalysis within

169 host-6, which forms a molecular cube in solution from eight Co<sup>II</sup> atoms and twelve ligands (**Figure**

170 **1f**). This host has an overall cationic charge of 16<sup>+</sup>, which enables it to bind anions such as chloride,

171 fluoride and hydroxide to its surfaces in water. The host is an efficient catalyst for the Kemp

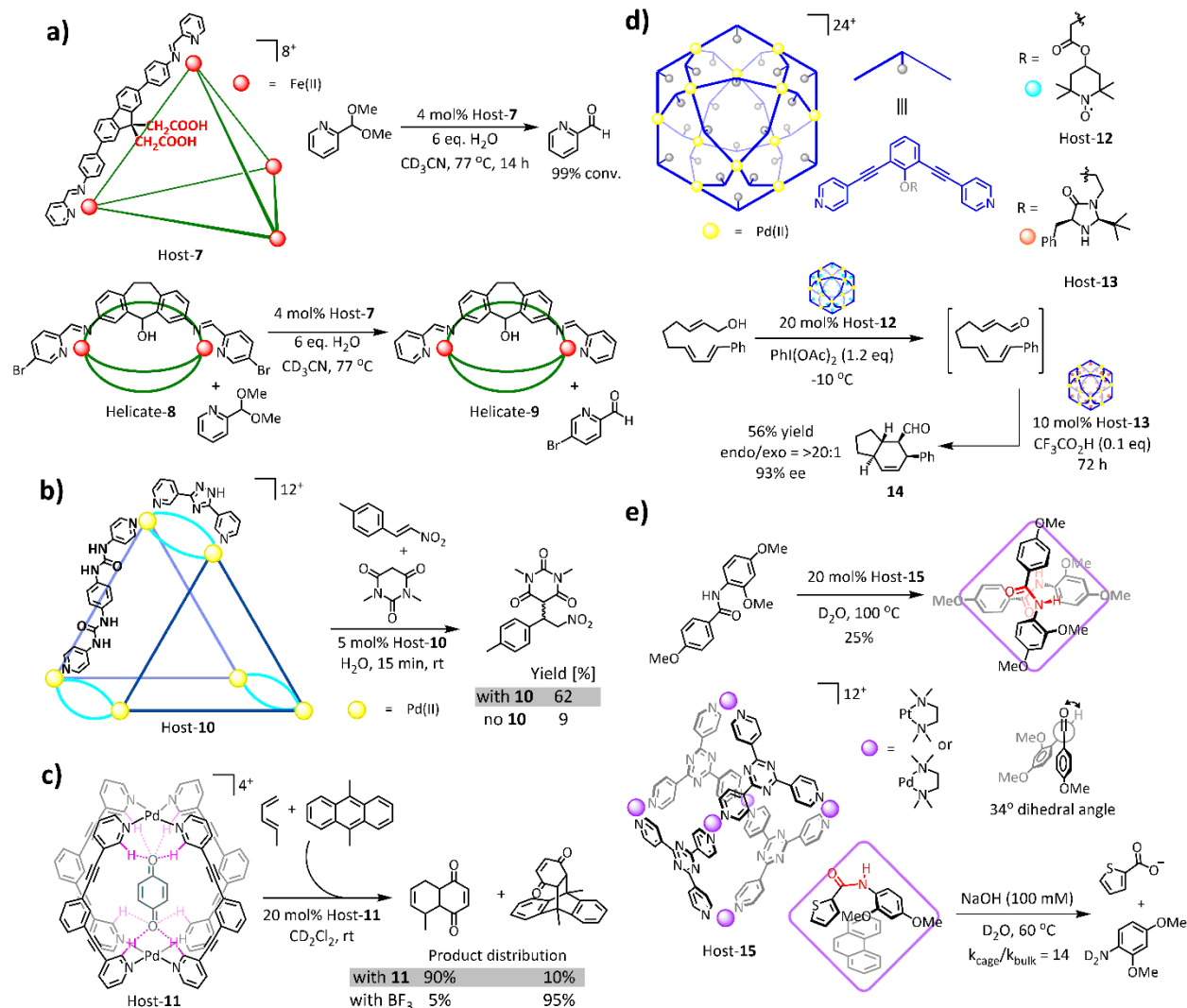
172 elimination of benzisoxazole to 2-cyanophenolate, with  $2 \times 10^5$  rate acceleration.<sup>51</sup> This elimination  
173 reaction is facilitated by an increase in local concentration of hydroxide ions around the host. In  
174 addition, this reaction is autocatalytic in the absence of a strong base, as the phenolate ion  
175 generated in the Kemp elimination binds to the outer face of the host, deprotonating an equivalent  
176 of starting material.<sup>52</sup>

177 In addition to increasing the local activity (in the thermodynamic sense) of reactive species  
178 such as hydroxide, supramolecular hosts have also been designed with specific activating groups  
179 for enabling catalysis. One such example is host-7 reported by Hooley and co-workers, which  
180 contains endohedral carboxylic acids for the purpose of enabling Brønsted acid catalysis.<sup>53</sup> Host-  
181 7 is an efficient catalyst for acetal deprotection, giving high conversions even in neutral water  
182 (**Figure 2a**). By compartmentalizing the Brønsted acid source, this cage enabled a multistep, one-  
183 pot synthesis with acid-sensitive reagents such as imine-based helicate-8. Helicate-8 underwent  
184 ligand substitution with pyridyl aldehydes that are *in situ* deprotected by host-7, to give non-  
185 brominated helicate-9. Another example of a host containing activating groups for catalysis is the  
186 supramolecular trigonal prism synthesized by Mukherjee and coworkers.<sup>54</sup> Host-10 self-assembles  
187 from six equivalents of urea-containing pyridyl ligands, six equivalents of Pd<sup>II</sup>, and six equivalents  
188 of a shorter ligand to “clip” the supramolecular prism together (**Figure 2b**). Hydrogen bonding  
189 interactions from the urea functionalities activated Michael additions of nitro-olefins to 1,3-  
190 dimethylbarbituric acid and Diels-Alder reactions of anthracene at 5 mol% loading of the catalyst  
191 in water. In the absence of host, little to no reactivity was observed. In another example of a host  
192 containing activating functionalities, Lusby and co-workers synthesized Pd<sup>II</sup> helicate host-11,  
193 designed to activate dienophiles for chemoselective Diels-Alder reactions (**Figure 2c**).<sup>55</sup> This host  
194 contains two distal hydrogen bonding sites at the polarized *ortho*-C–H bonds of the Pd-bound

195 pyridine, which selectively bind and activate *para*-quinone. With 20 mol% host-**11**, 1,3-pentadiene  
196 underwent a chemoselective Diels-Alder reaction with *p*-quinone, even in the presence of a  
197 competing diene, anthracene.

198 Multi-cage systems with preinstalled activating groups can also promote a multi-catalyst,  
199 one-pot, cascade reaction. Fujita and co-workers reported hosts **12** and **13** as catalysts for a tandem  
200 oxidation-Diels-Alder reaction (**Figure 2d**).<sup>56</sup> Host-**12** contains pendant oxidation catalyst  
201 TEMPO, while host-**13** contains a chiral amine Diels-Alder catalyst for enones. This chiral amine  
202 is incompatible with TEMPO in bulk solution, but within host-**13**, the amine is physically  
203 separated from the oxidation catalyst imbedded in host-**12**. This two-cage system oxidized an  
204 allylic alcohol to the corresponding  $\alpha,\beta$ -unsaturated aldehyde, which underwent selective  
205 cyclization to Diels-Alder adduct **14** with high ee in host-**13**. This example highlights the capability  
206 of synthetic hosts to mimic cascade reactions found in enzymatic systems, enabling multi-step  
207 transformations to occur in a single pot.

208 A recent report by Fujita and co-workers presents another way to generate reactivity within  
209 a host: by accessing mechanically strained intermediates.<sup>57</sup> The Pt<sup>II</sup> based host-**15** encapsulated  
210 two equivalents of aromatic amides in a *cis*-twisted conformation with up to a 34-degree dihedral  
211 angle between the carbonyl and N-H bond (**Figure 2e**). This conformation disrupts the stabilizing  
212 resonance interactions within the amide bond, causing these encapsulated amides to hydrolyse  
213 faster than observed for the free *trans* isomer. On subjecting the host-guest system to basic  
214 conditions, the twisted *s-cis* conformer hydrolysis was accelerated up to 14-fold. This example  
215 demonstrates the ability for supramolecular hosts to destabilize ground states to accelerate  
216 reactions.



217

## 218 Figure 2: Organic transformations promoted by supramolecular hosts

219 **a)** Acetal hydrolysis catalysed by acid functionalized host-7, followed by helicate substitution  
 220 reaction to generate helicate-9. **b)** Self-assembled host-10 containing urea activating groups, and  
 221 the 1,4-addition to nitro-olefins, promoted by the urea functionalities. **c)** Supramolecular host for  
 222 a catalytic Diels-Alder reaction, illustrating the selectivity for the smaller diene in the Diels-Alder  
 223 reaction with *para*-quinone. **d)** Tandem reaction catalysed by hosts **12** and **13** to generate Diels-  
 224 Alder adduct **14** selectively in one pot. **e)** Top: Encapsulation of aryl amides enforces a twisted-  
 225 *cis* conformation within host-15. Bottom: The twisted-*cis* conformation of encapsulated amides  
 226 accelerates hydrolysis.

227

228

229

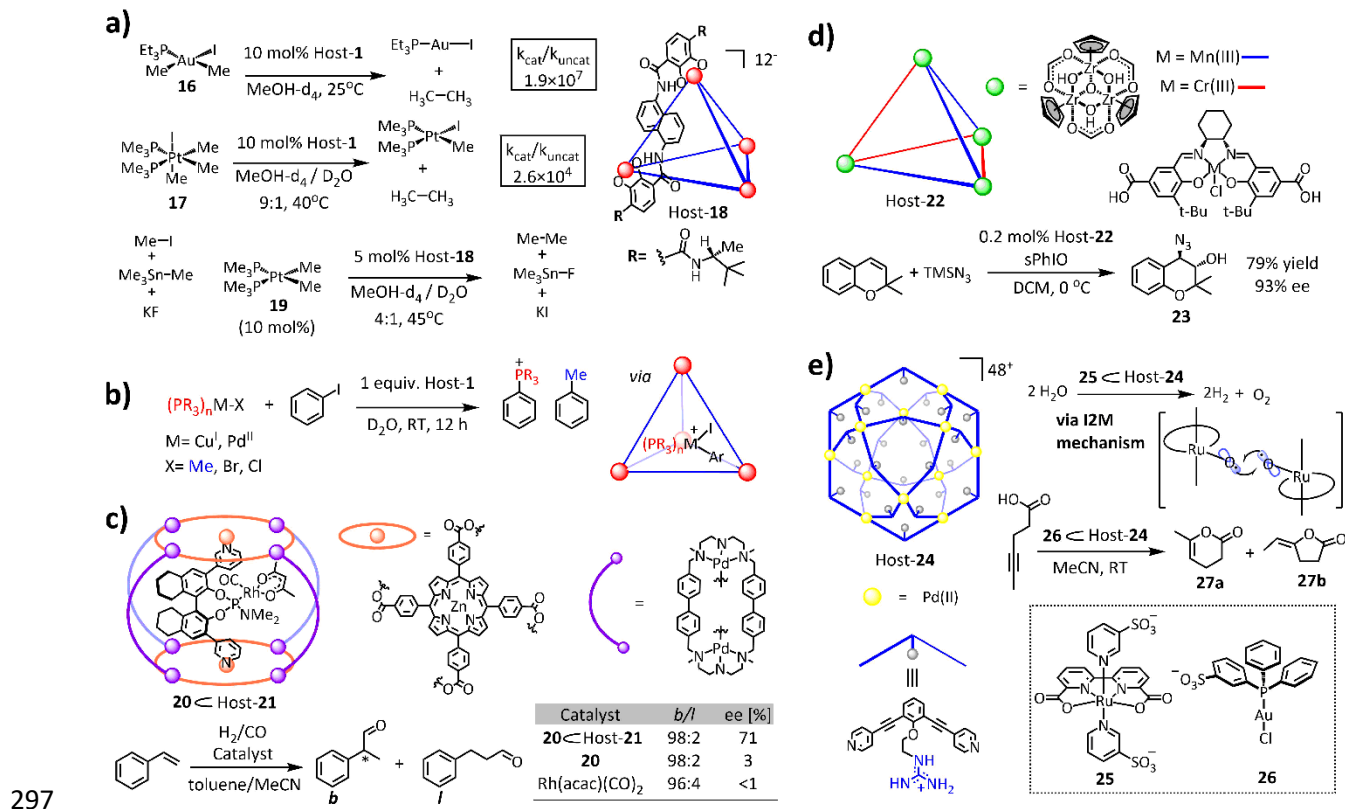
## 230 Organometallic Reactions Catalysed by Supramolecular Hosts

231 Supramolecular hosts enable novel reactivity for organometallic catalysts in ways  
232 otherwise inaccessible by traditional ligand scaffolds, much as proteins can alter the secondary  
233 coordination sphere in enzymes. Charged hosts can stabilize oppositely charged reaction  
234 intermediates to accelerate or favour a particular reaction pathway, as highlighted by the  
235 acceleration of elementary organometallic steps within the anionic tetrahedral host-**1** studied by  
236 the Raymond, Bergman and Toste groups (**Figure 1a**).<sup>58</sup> Host-**1** catalysed the reductive  
237 elimination of a dimethyl monophosphine Au<sup>III</sup> iodide (**16**) to form ethane with a  $1.9 \times 10^7$ -fold rate  
238 acceleration (**Figure 3a**).<sup>59</sup> This dramatic rate acceleration has been attributed to constrictive  
239 binding and stabilization of the positively charged transition state by the anionic host.<sup>60</sup> Similarly,  
240 the rate of reductive elimination from an encapsulated Pt<sup>IV</sup> complex (**17**) was increased  $2.6 \times 10^4$ -  
241 fold (**Figure 3a**). Host-**1** has a turnover number (TON) of 312 for the reductive elimination from  
242 **16**, but this TON was increased to 947 for related host-**18**, which is made more stable to alkyl  
243 halides by chiral amides at its vertices. Host-**18** behaved as a cocatalyst with platinum complex **19**  
244 in a dual catalytic mechanism for the  $sp^3$ - $sp^3$  cross coupling of an alkyl tin and alkyl halide,  
245 accelerating the prohibitively slow reductive elimination step of the catalytic cycle (**Figure 3a**).<sup>61</sup>  
246 Notably, this represents a unique example in which an organometallic complex shuttles between  
247 cooperative catalytic cycles occurring both inside and outside of the host cavity. Host-**1** also  
248 accelerates  $\beta$ -hydride elimination from an ethyl dimethyl Pt<sup>IV</sup> complex to form ethylene, and  
249 reductive elimination from an acyl dimethyl Pt<sup>IV</sup> complex to yield acetone. The scope of this  
250 system is limited by the size of the host cavity, which excludes a larger benzyl dimethyl Pt<sup>IV</sup>  
251 complex.

252 Besides acceleration of reductive elimination, host-1 likewise accelerates oxidative  
253 addition. Host-1 promoted the oxidative addition of aryl halides to encapsulated Cu<sup>I</sup> and Pd<sup>II</sup>  
254 complexes (**Figure 3b**).<sup>62</sup> Control experiments showed that these oxidative additions occur  
255 uniquely within the host, as the metal complexes are either unreactive or follow decomposition  
256 pathways in its absence. Reaction selectivity was also altered due to the confined nature of the  
257 cavity microenvironment—*para*-iodotoluene is typically more reactive toward oxidative addition  
258 than *ortho*- and *meta*-iodotoluene, but this trend was reversed under host-mediated reaction  
259 conditions, due to the sterically-limited binding affinity of *para*-iodotoluene. These results  
260 highlight the ability of supramolecular hosts not only to accelerate the elementary steps of  
261 organometallic catalysis but also to exhibit atypical selectivity resulting from differential binding.

262 Supramolecular hosts have also demonstrated the ability to enhance enantioselective  
263 transformations induced by single metal catalysts. Notably, Reek and co-workers reported an  
264 enantioselective hydroformylation reaction for branched aldehyde products, catalysed by a  
265 supramolecular Rh complex.<sup>63</sup> Catalyst-20 consists of a Rh-ligated chiral phosphoramidite, which  
266 is coordinated to a mixed Zn<sup>II</sup> porphyrin and Pd-based coordination host (**Figure 3c**). 20⊂Host-  
267 21 provided up to 71% ee and high conversion to the branched product, significantly out-  
268 performing the free phosphoramidite Rh catalyst. Cui and co-workers also reported highly  
269 enantioselective catalysis with host-22 (**Figure 3d**). Host-22 self-assembles from three equivalents  
270 of chiral Cr- and Mn-salen based ligands and Zr vertices.<sup>64</sup> This multi-metal host catalysed the  
271 tandem epoxidation and nucleophilic ring opening to give product 23 in high conversions and  
272 enantioselectivity. While the host did not increase the inherent ee provided by the free Mn-salen  
273 catalyst, it led to increased overall conversions. This example thus highlights the ability of  
274 supramolecular hosts to stabilize catalysts at lower loadings and increase their TON.

275 In addition to providing rate acceleration to mononuclear catalysts, supramolecular hosts  
276 have demonstrated the ability to pre-organize multiple metal catalysts and enhance their catalytic  
277 behaviour, as shown by Reek and co-workers. Through hydrogen bonding interactions between  
278 host-bound guanidinium moieties and pyridine-bound sulphate moieties, host-**24** can encapsulate  
279 up to twelve pyridine-ligated ruthenium complexes (**25**), creating a local ruthenium concentration  
280 of up to 0.54M within its cavity—a condition difficult to attain in bulk solution due to solubility  
281 and cost considerations (**Figure 3e**).<sup>65</sup> The host-catalyst complex accelerated electrochemical  
282 water oxidation by two orders of magnitude through facilitation of the rate-limiting step, dinuclear  
283 coupling of molecular oxygen, which was favoured by the increased local concentration of catalyst  
284 (**Figure 3e**). Similarly, host-**24** can bind up to twelve copper Xantphos-based catalysts, modified  
285 to contain sulphate groups to interact with the host, and accelerate the copper-catalysed cyclization  
286 of 4-pentynoic acid.<sup>66</sup> This reaction also involves a rate-limiting dinuclear coupling step, which  
287 was accelerated 50-fold despite the low average concentration of catalyst in solution. Additionally,  
288 the host increased the turnover number by 2.5-fold compared to the unencapsulated copper catalyst  
289 under the same reaction conditions. In a recent study, host-**24** not only pre-organized gold catalyst  
290 **26**, but the substrate as well in the intramolecular cyclization of acetylenic acids (**Figure 3e**).<sup>67, 68</sup>  
291 Aided by the addition of catalytic base, interactions between the substrate's deprotonated  
292 carboxylic acid groups and the host's guanidinium groups led to selective formation of a five-  
293 membered ring (**27b**) over a six-membered ring (**27a**), which was favoured in absence of the host.  
294 Conversion decreased when the number of encapsulated gold complexes in each host cavity  
295 exceeded four, as binding sites for the substrate were blocked, further evidencing the influence of  
296 host-induced conformational pre-organization.



298 **Figure 3: Organometallic transformations promoted supramolecular hosts**

299 **a)** Reductive elimination of Au<sup>III</sup> and Pt<sup>IV</sup> catalysed by host-1, and dual catalytic reaction for sp<sup>3</sup>-  
 300 sp<sup>3</sup> cross coupling to give ethane catalysed by Pt<sup>IV</sup> and host-18. **b)** Oxidative addition of aryl  
 301 halides to Cu<sup>I</sup> and Pd<sup>II</sup> catalysed by host-1. **c)** Top: Chiral phosphoramidite Rh catalyst **20**  
 302 encapsulated by host-21. Bottom: hydroformylation conditions highlighting the enhanced  
 303 selectivity for the encapsulated catalyst over the free Rh catalyst **20**. **d)** Top: Chiral salen-based  
 304 tetrahedral host-22. Bottom: Conditions for the tandem asymmetric epoxidation, azide addition  
 305 reaction catalysed by Host-22. **e)** Left: Host-24 containing endohedral guanidinium functionalities.  
 306 Right: Dinuclear Ru water oxidation and dinuclear Au cycloisomerization promoted by host-24.

307 Supramolecular hosts have also proven useful in metal nanoparticle and nanocluster  
 308 catalysis. The host cavity provides a protecting scaffold for the formation of uniform nanoclusters,  
 309 improving catalytic performance and preventing decomposition, agglomeration, or other  
 310 disorganizing pathways. In one example, Chen and co-workers reported a trigonal prismatic  
 311 coordination cage with thiophene ligands that bind Pt<sup>IV</sup> precursors to form Pt<sup>0</sup> nanoclusters, which  
 312 demonstrated higher electrocatalytic performance than Pt/C for the hydrogen evolution reaction

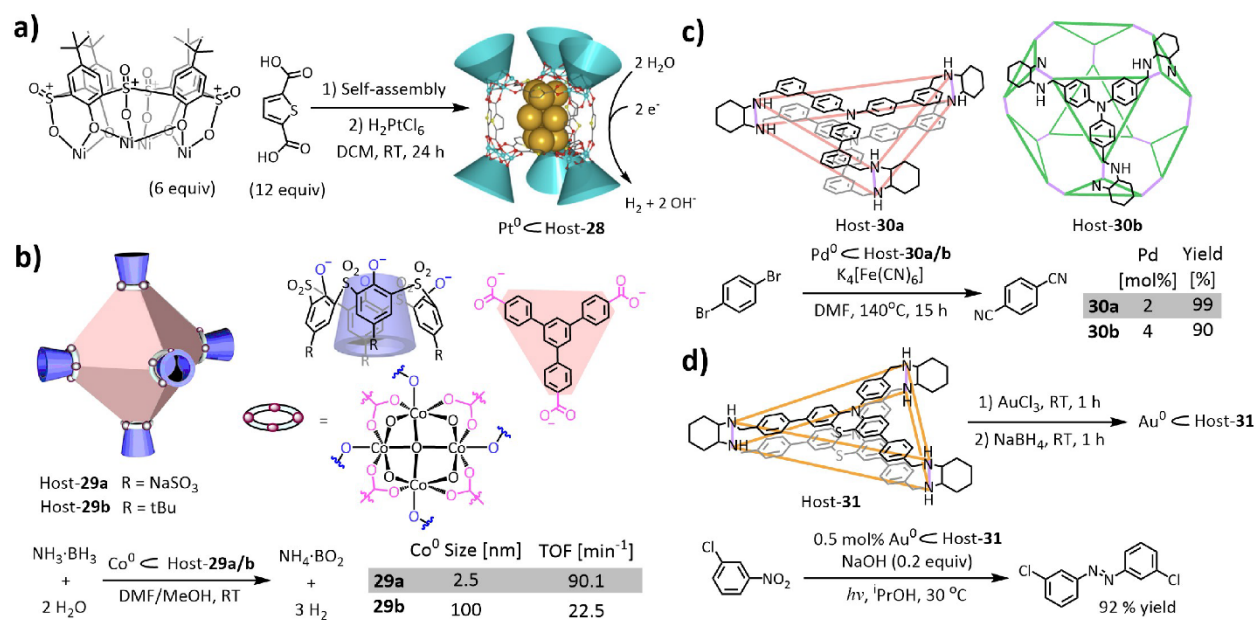


313 (HER) (**Figure 4a**).<sup>69</sup> Host-**28** had higher current density, longer durability, and stronger corrosion  
314 resistance than Pt/C.

315 The Zhou group also reported a porous coordination cage (host-**29**) that encapsulates metal  
316 cations in solution, which were reduced to form neutral metal nanoclusters within its pores.  
317 Composite cobalt nanoclusters within host-**29a** showed superior catalytic activity in the hydrolysis  
318 of ammonia-borane compared to other first row transition metal nanocluster catalysts (**Figure**  
319 **4b**).<sup>70</sup> The negatively charged host-**29a** coordinates and organizes Co<sup>II</sup> cations into smaller and  
320 more uniform particles within its cavity, preventing the detrimental agglomeration of the particles,  
321 even after reduction to Co<sup>0</sup>. The significance of charge was evidenced by comparison to an overall  
322 neutral analogue, host-**29b**, in which the sulphate groups were replaced with tert-butyl groups,  
323 leading to instant agglomeration, followed by slower reaction times and slower turnover frequency  
324 (**Figure 4b**). Zhou and co-workers also reported encapsulation of Ru<sup>III</sup> cations in host-**29a** to form  
325 uniform Ru<sup>0</sup> nanoclusters with improved catalytic activity in the methanolysis of ammonia  
326 borane.<sup>71</sup> These examples highlight the possibilities of cooperation between supramolecular  
327 chemistry and metal nanoparticles for small molecule catalysis.

328 In another instance of supramolecular nanoparticle catalysis, Mukherjee and co-workers  
329 reported host-**30a** and host-**30b**, with multiple interior diamine binding sites that aid in the  
330 synthesis of Pd<sup>0</sup> nanoparticles. The nanoparticles exhibited improved stability and catalytic  
331 performance in the cyanation of aryl halides compared to other common palladium catalysts  
332 (**Figure 4c**).<sup>72</sup> Host-**30a** has a significantly smaller cavity than host-**30b**, which led to the  
333 formation of smaller Pd nanoparticles. As a result, host-**30a** demonstrated superior catalytic  
334 activity, evidencing the influence of supramolecular hosts through modulation of particle size.  
335 Another covalent organic cage (host-**31**) reported by Mukherjee and co-workers promoted the

336 formation of Au<sup>0</sup> nanoparticles within its cavity, which act as heterogeneous photocatalysts for the  
 337 conversion of nitroarenes to their corresponding azo- compounds (**Figure 4d**).<sup>73</sup> Host-**31** contains  
 338 photosensitizing phenothiazines, and prevented the agglomeration of the gold nanoparticles by  
 339 regulating particle size, which improved their photocatalytic activity and reusability. Catalysis  
 340 proceeded under mild conditions with >99% selectivity for the azo-product, followed by easy  
 341 separation of the catalyst (**Figure 4d**). In summary, supramolecular hosts show great potential in  
 342 transition metal catalysis, enhancing the catalytic abilities of the metal through electrostatic  
 343 stabilization, pre-organization, and protection from degradation pathways.



344

### 345 **Figure 4: Host mediated metal nanoparticle synthesis and reactivity**

346 **a)** Self-assembly of host-**28** reported by Chen and workers, which catalyses hydrogen evolution  
 347 reaction (HER) through encapsulated Pt<sup>0</sup> nanoclusters. **b)** Top: anionic and neutral hosts **29a/b**  
 348 self-assembled from three components. Bottom: Conditions for oxidation of borane catalysed by  
 349 metal nanoclusters within host-**29a/b**. **c)** Top: two differently-sized covalent cages synthesized by  
 350 Mukherjee and co-workers. Bottom: Conditions for cyanation catalysed by Pd<sup>0</sup> nanoparticles  
 351 within hosts **30a** and **30b**. **d)** Top: phenothiazine-containing covalent cage synthesized by  
 352 Mukherjee and co-workers. Bottom: azo-formation reaction catalysed by gold particles within  
 353 host-**31**, which also acts as a photosensitizing agent.

354

355

## 356 **Regio- and Site-Selective Reactivity Enabled by Supramolecular Hosts**

357 Reactions made regio- or site-selective by supramolecular catalysis represent ongoing  
358 efforts toward bridging the gap between proof-of-concept reactivity and synthetic application. For  
359 these reactions the primary purpose of the host is not to provide overall rate acceleration, but  
360 instead a secondary sphere in which selective binding and guest recognition promote a significant  
361 rate differential between desired and competing undesired reaction trajectories. Two general  
362 approaches have been undertaken to attain this supramolecular-controlled selectivity. The first  
363 approach uses the host as a stoichiometric supramolecular “protecting group” to bind lipophilic  
364 portions of the substrate, while the reactive species is directed to a distal portion of the substrate  
365 *outside* of the host. The second approach involves the encapsulation of a transition metal catalyst,  
366 which provides a secondary environment to direct chemo and regioselectivity *inside* the host.

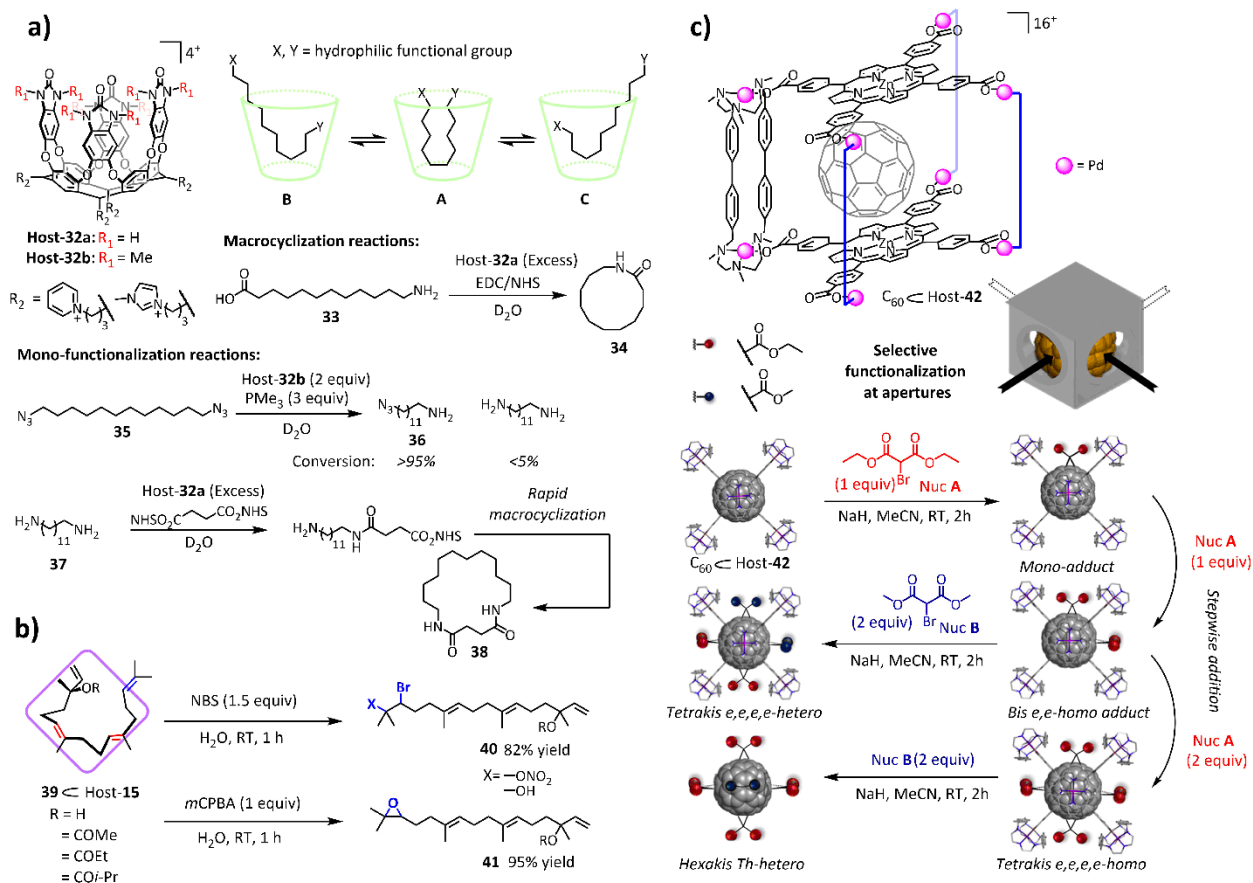
367 The Rebek group has been a leader in implementing the first approach, exemplified by the  
368 selective macrocyclization and mono-functionalization reactions mediated by cavitand host-**32a/b**  
369 (**Figure 5a**).<sup>74–80</sup> The deep pocket formed by the aromatic scaffold enables strong hydrophobic  
370 binding to the lipophilic portion of bolaamphiphiles such as  $\alpha$ ,  $\omega$ -amino acid **33**.<sup>75</sup> When bound,  
371 the substrate adopts a U-shaped conformation, projecting the polar, reactive end groups close  
372 together at the solvent-exposed rim (**A**). Upon subjecting this system to conventional amide-bond  
373 forming conditions using NHS (N-hydroxysuccinimide) and EDC (N-ethyl-N'-(3-  
374 dimethylaminopropyl)carbodiimide), the corresponding cyclic lactam product **34** was selectively  
375 observed. In the absence of super-stoichiometric host-**32a**, oligomeric products formed despite  
376 high-dilution conditions, indicating that the host not only reduces the entropic barrier of  
377 macrocyclization, but functions as a sterically-hindered protecting group to prevent intermolecular  
378 reactivity. Similar reactivity was observed with  $\alpha$ ,  $\omega$ -dienes, in which host-**32a** facilitated an

379 intramolecular olefin-metathesis reaction leading to the selective formation of cyclooctene in the  
380 presence of Hoveyda-Grubbs-II catalyst.<sup>76</sup> This system was extended to the mono-  
381 functionalization reaction of difunctional alkanes by subjecting  $\alpha$ ,  $\omega$ -diazide **35** to Staudinger  
382 reduction conditions in the presence of stoichiometric quantities of N-methyl urea cavitand, host-  
383 **32b**.<sup>77</sup> Remarkably, mono-reduction product **36** was exclusively formed, even with excess  
384 phosphine, whereas a mixture of reduction products form in the absence of the host. This  
385 selectivity is attributed to a shift in the equilibrium towards conformation **B/C** upon mono-  
386 reduction, where the amine extrudes from the cavity and the more lipophilic azide is shielded from  
387 further reduction. Selective mono-functionalization and macrocyclization was also accomplished  
388 successively in a one-pot fashion, as shown by the host-**32a** mediated transformation of diamine  
389 **37** to di-lactam **38**.<sup>80</sup>

390 Fujita and co-workers extended this supramolecular “protecting group” approach further  
391 by investigating its application to a simple natural product (**Figure 5b**).<sup>81</sup> Previously reported Pd  
392 host-**15** (**Figure 2e**) self-assembles from four triazole ligands, forming a highly hydrophobic,  
393 octahedral cavity. Geranylinalool **39** forms a 1:1 inclusion complex with host-**15** under aqueous  
394 conditions in which it adopts a U-shaped conformation, evidenced both by <sup>1</sup>H-<sup>1</sup>H NOESY  
395 correlation experiments and X-ray crystallography. The terminal prenyl moiety extrudes from the  
396 cavity, whereas the two internal trisubstituted double bonds are well-encapsulated. Subjecting  
397 host-guest complex **39**⊂**15** to an aqueous solution of N-bromosuccinimide (NBS) yielded a single  
398 product, with exclusive bromination at the exposed prenyl site. Subsequent bromonium ring-  
399 opening by NO<sub>3</sub><sup>-</sup> counterions formed 14,15-nitratobrominated product **40** in 82% yield. Control  
400 experiments in the absence of the cage yielded a mixture of bromination products due to competing  
401 reactivity at the internal (10, 11) alkenyl group. High site-selective reactivity was also observed

402 upon addition of *m*-chloroperoxybenzoic acid to **39****C15**, where epoxidation occurred exclusively  
403 at the prenyl end group to give product **41** in quantitative yield.

404 While the previous examples demonstrated modification of a single, solvent-exposed site,  
405 a recent report from Ribas and co-workers presents a modular approach that enables access to a  
406 range of selectively modified fullerene products.<sup>82</sup> Controlled functionalization of C<sub>60</sub> is an  
407 important challenge in the design of improved perovskite thin layers in solar cell devices.  
408 Tetragonal prismatic host-**42**, consisting of two Zn<sup>II</sup>-porphyrin moieties and four Pd<sup>II</sup>-molecular  
409 clips, was previously reported to form 1:1 inclusion complex C<sub>60</sub>**C42** in acetonitrile.<sup>83</sup> While fully  
410 encapsulated, portions of the guest remain exposed to the solvent through four lateral apertures  
411 (**Figure 5c**). Subjecting C<sub>60</sub>**C42** to standard Bingel-Hirsch conditions with one equivalent of ethyl  
412 bromomalonate (Nuc **A**) resulted in the formation of the regioisomerically pure mono-adduct,  
413 where cyclopropanation occurred exclusively at a solvent-exposed, equatorial [6,6] bond.  
414 Subsequent additions of Nuc **A** resulted in the stepwise formation of bis-, tris-, and tetrakis-  
415 equatorial *homo*-adducts, and addition of methylmalonate (Nuc **B**) enabled formation of the  
416 corresponding *hetero*-adducts, showcasing the modularity of this strategy.



417

418 **Figure 5. Regio- and site-selective reactivity rendered by stoichiometric amounts of**  
 419 **supramolecular hosts**

420 **a)** Top left: Cavitaand host-**32a** synthesized by Rebek and co-workers. Top right: Binding equilibria  
 421 within host-**32**, showing yo-yo like motion. Bottom: Macrocyclization and mono-functionalization  
 422 reactions facilitated by stoichiometric encapsulation in host-**32a/b**. **b)** Quantitative encapsulation  
 423 of diterpenoid renders site-selective electrophilic bromination and epoxidation outside the cage. **c)**  
 424 Top: Tetragonal prismatic host-**42** synthesized by Ribas and co-workers. Bottom: Stepwise  
 425 addition of bromomalonate nucleophiles renders modular site-selective Bingel-Hirsch  
 426 cyclopropanations.

427 The supramolecular protecting group approach enables high levels of selectivity across  
 428 different host-guest platforms and organic reactions, but its application requires quantitative  
 429 formation of the host-guest complex and super-stoichiometric concentrations of host, which can  
 430 limit its scope and scalability. An alternative approach that promotes high selectivity at catalytic  
 431 loading of host involves anchoring a reactive metal catalyst internally, thereby restricting the size  
 432 and conformations of substrates that can co-encapsulate. Host-**43a**-catalyzed regioselective

433 hydroformylation, first reported by Reek and co-workers in 2001, is a well-established  
434 example.<sup>63,84–89</sup> Host-**43a** self-assembles from three Zn<sup>II</sup>-tetraphenylporphyrin (Zn-TPP) moieties  
435 that coordinate to the pyridyl units of tris(*m*-pyridyl)phosphine (**Figure 6a**). Addition of a Rh<sup>I</sup>  
436 precursor results in the formation of an encapsulated mono-phosphine Rh complex, an active  
437 catalyst in the hydroformylation of 1-octene. While the free Rh complex was selective for the  
438 linear aldehyde product, the [Rh]⊂**43a** complex reversed selectivity, forming the branched product  
439 in larger quantities ( $l/b < 1$ ). In a subsequent study, the size of the cage was modulated to further  
440 elucidate the effect of confinement on the selectivity of the reaction.<sup>85</sup> Smaller host-**43b** was  
441 synthesized by replacing the Zn-TPP ligands with electron-deficient tetraphenylporpholactone  
442 (Zn-TPPL), which resulted in a stronger and shorter Zn-pyridyl interaction and a calculated 44%  
443 decrease in cavity volume compared to **43a**. In parallel hydroformylation reactions of 1-octene  
444 and propene, host-**43a** exhibited a higher  $b/l$  ratio for 1-octene, whereas host-**43b** was more  
445 selective for propene. These observations are attributed to match/mismatch effects, where the  
446 smaller host-**43b** is configurationally “matched” with the smaller propene substrate, and **43a** with  
447 the larger octene. Modular reactivity can thus be achieved by fine-tuning the steric and electronic  
448 properties of the supramolecular coordination sphere.

449 In another example by Reek, Nitschke, and co-workers, a Rh hydroformylation catalyst  
450 was encapsulated within host-**44**, a zinc-porphyrin analogue of a previously reported Fe<sub>4</sub>L<sub>6</sub> host  
451 (**Figure 6b**).<sup>87</sup> The cage assembles around two phosphine ligands, which together chelate a single  
452 Rh complex. Upon subjecting a series of terminal olefins to supramolecular hydroformylation  
453 conditions, smaller substrates (1-hexene) underwent significantly higher conversions than larger  
454 substrates (styrene). Control reactions in the absence of **44** showed a narrower range of conversions

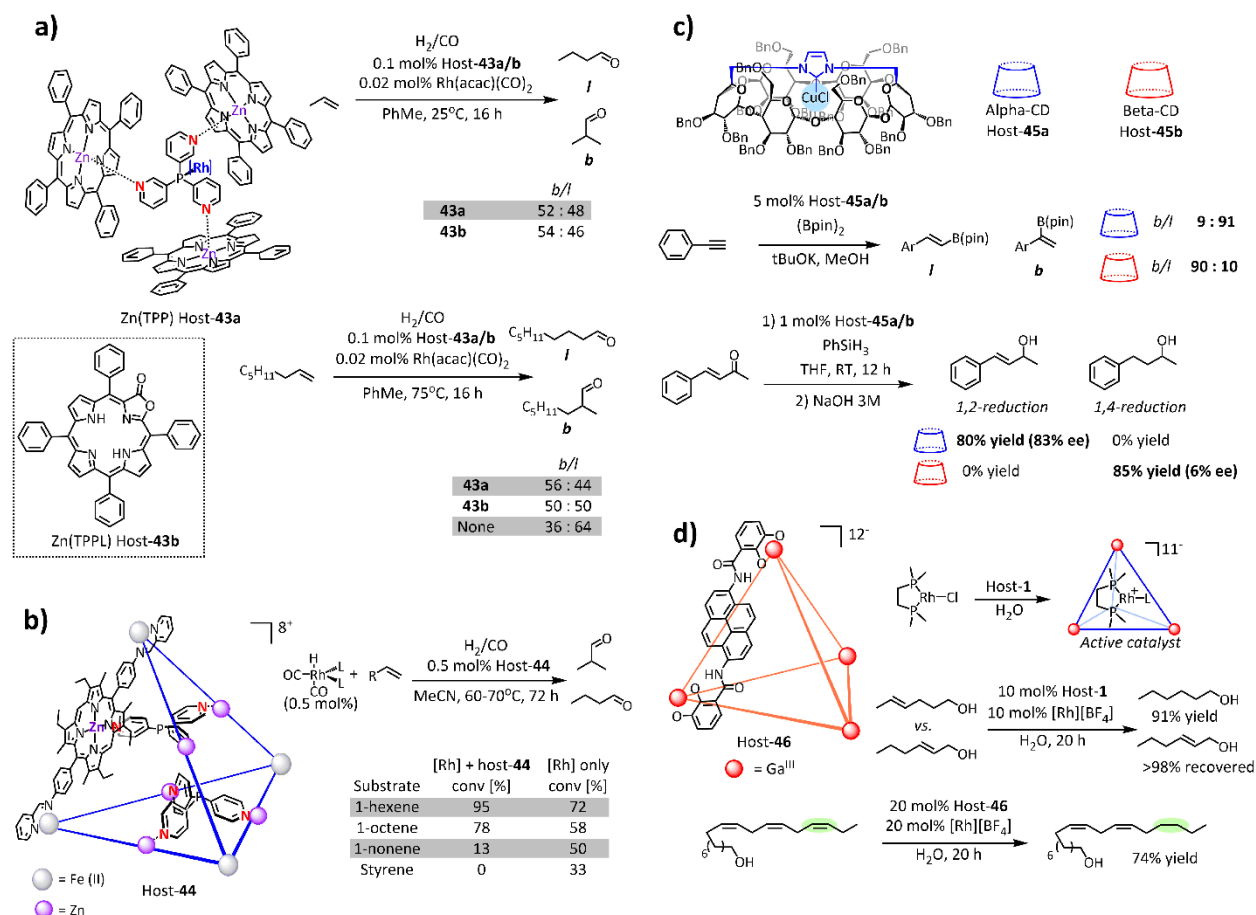
455 regardless of substrate size. This example demonstrates that supramolecular host-mediated  
456 regioselectivity can be extended to size-selective transformations as well.

457         While previous examples involved multi-component syntheses of novel supramolecular  
458 hosts, Sollogoub and co-workers demonstrated regioselective reactivity using covalent *N*-  
459 heterocyclic carbene (NHC)-capped  $\alpha$ -cyclodextrin host-**45a** and  $\beta$ -cyclodextrin host-**45b** (**Figure**  
460 **6c**).<sup>90</sup> NHC coordination to Cu<sup>I</sup>Cl creates an active encapsulated catalyst for the borylation of  
461 phenylalkynes.<sup>91</sup> Subjecting substituted and unsubstituted terminal and internal phenylalkynes to  
462 host-**45a**-mediated borylation conditions resulted in excellent selectivity for the linear products,  
463 yielding *b/l* ratios as low as 0.02. In contrast, the larger host-**45b** catalysed the formation of the  
464 branched product as the major isomer under otherwise identical conditions. NMR studies of the  
465 reaction intermediates revealed that the selectivity-determining *syn*-borylcupration step occurs  
466 within the host cavity. DFT analyses suggested that the smaller cavity size of **45a** enforces an  
467 orthogonal, horizontal approach of the acetylene, whereas **45b** promotes a vertical approach, in  
468 which the alkyne projects directly into the larger cavity.

469         In another example by Sollogoub and co-workers, host-**45a/b** were utilized in the  
470 regioselective hydrosilylation of conjugated enones (**Figure 6c**).<sup>92</sup> The generation and stabilization  
471 of a distinct, monomeric Cu-H species within the host cavity enabled asymmetric reduction of  
472 acetophenone in good yields and enantiomeric excess using phenylsilane as the reductant.  
473 Furthermore, host-**45a** was selective for the 1,2-reduction product for benzylideneacetone  
474 derivatives, whereas the larger host-**45b** generated the 1,4-reduction product. This example again  
475 demonstrates the ability of the two cyclodextrin-based ligands to stabilize and select for different  
476 orientations of the substrate as it approaches the reactive metal centre.



477 While regioselective transformations at a single reactive site have been successfully  
478 demonstrated by encapsulated metal catalysts, site-selective reactivity in the presence of multiple  
479 reactive sites is a longstanding challenge. A recent report by Raymond, Bergman, and Toste and  
480 co-workers addresses this challenge by demonstrating a rare example of site-selective  
481 hydrogenation of poly-enols utilizing the Ga naphthalene host-1 (**Figure 6d**).<sup>93</sup> The active  
482 hydrogenation catalyst was formed *via* halide abstraction from (DMPE)RhCl and encapsulation of  
483 the resulting Rh cation. Under host-catalysed hydrogenation conditions, various hexen-1-ol  
484 substrates yielded high conversions of olefins in which the double bond is remote from the  
485 hydroxyl group (5- and 4-hexen-1-ol), but little to no conversions of more proximate double bonds  
486 (3- and 2-hexen-1-ol). In stark contrast, the free Rh catalyst resulted in quantitative conversion of  
487 all hexen-1-ol substrates, regardless of alkene position. Increased site-selectivity was attributed to  
488 the preferential binding of the more lipophilic alkyl end of the pendant alcohol substrate within  
489 the host. Similarly, a linolenic acid derivative underwent selective hydrogenation in the presence  
490 of larger pyrene-based host-46. These examples demonstrate the potential of encapsulated metal  
491 catalysis to address synthetic challenges in the selective functionalization of natural products and  
492 biomolecules.



493  
494

## Figure 6. Regio- and site-selective reactivity catalysed by supramolecular hosts

495 **a)** Left: Zn(TPP) host-43a and smaller Zn(TPPL) host-43b. Right: linear vs. branched  
 496 hydroformylation of 1-octene and propene, in which host-43a and 43b give different selectivities.  
 497 **b)** Left: Host-44 by Reek, Nitschke and co-workers, which integrates Zn porphyrin moieties into  
 498 Fe<sub>4</sub>L<sub>6</sub> cage previously reported by the Nitschke group. Right: Smaller substrates generally result  
 499 in higher conversion, though some anomalous conversions were observed for 1-heptene and 1-  
 500 decene. **c)** Top:  $\alpha$ - and  $\beta$ -cyclodextrin hosts-45a and 45b, a bridging covalently tether NHC  
 501 chelates a molecule of CuCl. Bottom: 45a and 45b gives opposite selectivity in a copper-catalysed  
 502 borylation and hydrosilylation. **d)** Left: Larger pyrene host-46 by Toste and co-workers. Right:  
 503 Active cationic Rh complex formed inside the cage selectively hydrogenates terminal olefins.

504

505

506

507

## 508 Photochemical Reactivity Enabled by Supramolecular Hosts

509 Photochemical reactions are notoriously difficult to control due to their intrinsically low  
510 reaction barriers upon excitation and highly reactive intermediates. Supramolecular hosts provide  
511 an opportunity to control such reactions through pre-organization of reactive species, and in some  
512 cases modifying the photophysical properties of participating reagents. Supramolecular chemistry  
513 has historically been used in conjunction with photochemistry—nearly three decades ago, Cram  
514 and co-workers used a hemicarcerand host to stabilize and characterize antiaromatic  
515 cyclobutadiene, formed through a photochemical 4 pi-electrocyclic ring closure from 2-pyrone,  
516 followed by a retro-[2+2] to release CO<sub>2</sub>.<sup>94</sup> More recently, a host-guest system was shown to  
517 enhance the yield and enantioselectivity in a similar organic photoreaction. Aitken and co-workers  
518 reported the photochemical 4 pi-electrocyclization of lactam **47** assisted by heterogenous β-  
519 cyclodextrin (**β-CD**) (**Figure 7a**).<sup>95</sup> The chiral **β-CD** formed a 1:1 complex with **47** in the solid  
520 state, and upon UV irradiation product **48** was obtained in 79% yield and 38% ee.

521 Supramolecular hosts can also promote steric control in bimolecular photochemical  
522 reactions. Since the early 2000s, Inoue and co-workers have investigated the ability of cyclodextrin  
523 hosts to enforce stereo- and enantioselectivity on the photochemical [4+4] cyclodimerization of  
524 anthracenes.<sup>96</sup> Cyclodextrins typically favour head-to-tail dimerization of 2-anthracenecarboxylate  
525 by encapsulating two anthracenes with their carboxylate groups protruding from either end of the  
526 host. Increasingly complex cyclodextrin derivatives have been prepared to mediate this reaction,  
527 some bearing substitution at the rims, and others covalently linked to cocatalysts. In recent years,  
528 the Yang group has utilized cyclodextrin derivatives to attain high stereo- and regiocontrol over  
529 anthracene dimerization. With 0.5 mol% Host-**49**, a γ-cyclodextrin tethered to a platinum  
530 photosensitizing complex, the syn-head-to-tail cyclodimer **50** was favoured with 31.4% ee and

531 61% conversion (**Figure 7b**).<sup>97</sup> The attached platinum photosensitizer allowed sensitization with  
532 visible light, while anthracene itself only absorbs in the higher energy ultraviolet region.  
533 Cyclodextrin hosts can also form 2:2 complexes with anthracene to favour nonclassical “slipped”  
534 anthracene dimerization between a central and edge ring. Functionalization of the cyclodextrin’s  
535 primary alcohol rim with cationic ammonium salts (Host-**51a/b**) promotes electrostatic  
536 interactions with the carboxylate groups on the anthracenes. As a result, head-to-tail slipped dimers  
537 **52** and **53** were preferentially formed in high yield (92-100%) over classical cyclodimers (**Figure**  
538 **7c**).<sup>98</sup> Additionally, the products were formed with 71% ee for **52** and 45% ee for **53**. Further  
539 stereocontrol was achieved with host-**54**, which consists of two  $\beta$ -cyclodextrins tethered together  
540 by a sulphide link, and selectively forms anthracene cyclodimer **55** with 100% ee (**Figure 7d**).<sup>99</sup>  
541 Selectivity for head-to-tail cycloaddition both with cyclodextrin and in bulk solution was reversed  
542 with the use of the bowl-shaped octa-acid cavitand, host-**4** (**Figure 1e**). Host-**4** has a single solvent-  
543 exposed opening while cyclodextrin has two, and projects both hydrophilic carboxylate ends in  
544 the same direction, promoting the formation of head-to-head cyclodimers **56** and **57** (**Figure 7e**).<sup>100</sup>

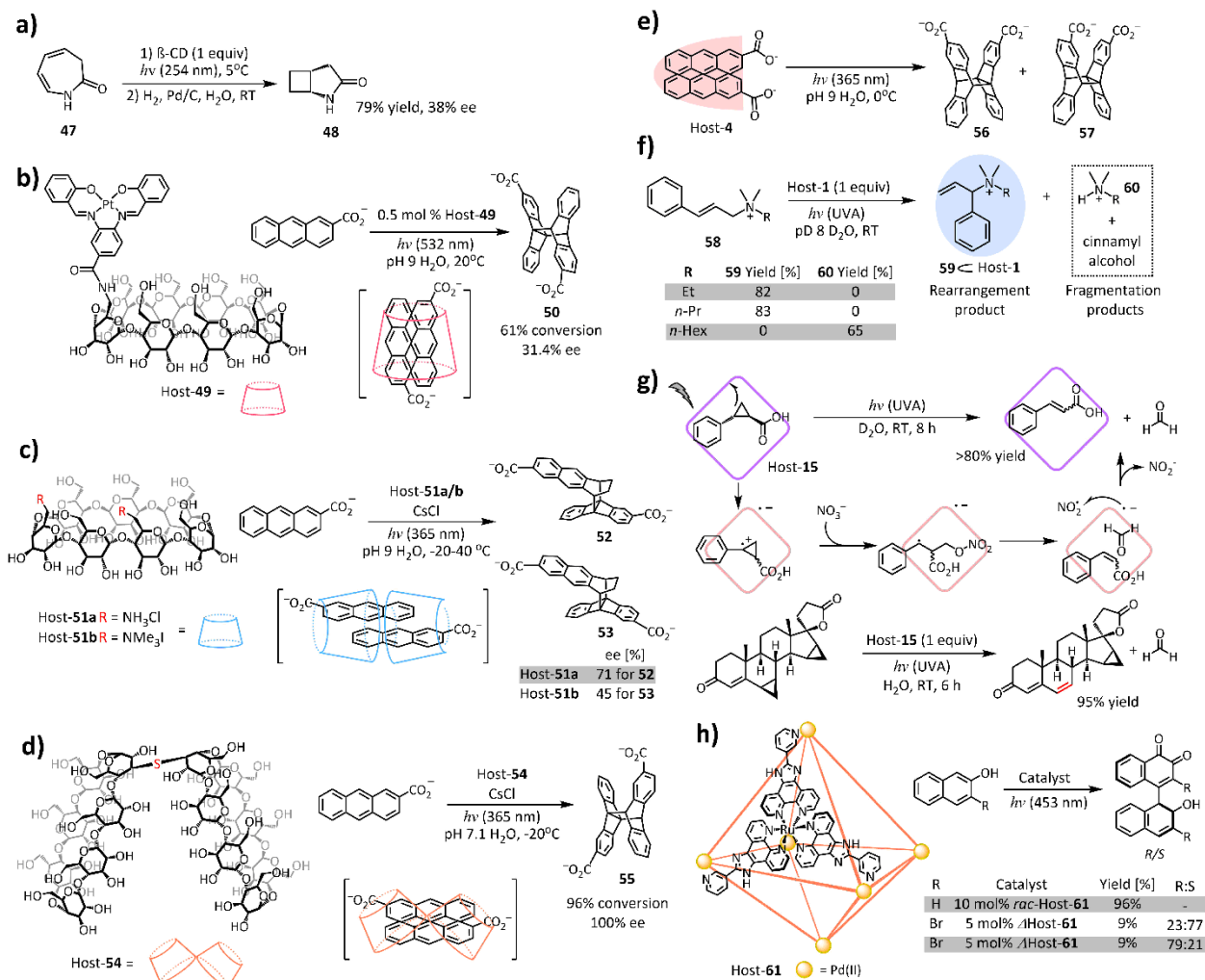
545 In addition to altering the stereochemical outcomes of photochemical transformations,  
546 redox-active supramolecular hosts can also function as photosensitizers to access otherwise  
547 challenging reactivity. The tris-catecholate tetrahedral host-**1** promoted a redox-neutral  
548 photochemical 1,3-rearrangement of allyl-dimethyl-cinnamylammonium derivatives (**58**) within  
549 its core via photoinduced electron transfer (PET) from its electron rich ligands (**Figure 7f**).<sup>101</sup> This  
550 rearrangement occurred in competition with a background fragmentation reaction, which arises  
551 from interception of the cinnamyl cation intermediate with water to give cinnamyl alcohol and  
552 dimethyl allyl amine. When the host was blocked by a competitive tetraethylammonium guest, no  
553 rearrangement product was observed, and fragmentation was the primary reaction pathway.

554 Stronger binding affinity of the starting material correlated with more rearrangement product (**59**),  
555 and conversely weaker binding affinity resulted in more fragmentation to cinnamyl alcohol and  
556 the corresponding amine (**60**). *N*-propyl and *N*-ethyl ammonium derivatives produced 83% and  
557 82% yield of rearrangement products respectively, whereas the weakly bound *N*-*n*-hexyl  
558 ammonium produced only fragmentation product. This reaction demonstrates how a host can not  
559 only photosensitize a reaction, but also provide access to alternative reaction trajectories through  
560 its confined cavity environment.

561 Fujita and co-workers have also reported a cyclopropane demethylenation photosensitized  
562 by a redox-active host (**Figure 7g**).<sup>102</sup> Host-**15** features an electron-deficient triazine ligand, which,  
563 upon irradiation, accepts an electron from the excited cyclopropane-containing guest. The resulting  
564 cyclopropyl radical cation is then proposed to undergo rapid ring-opening via nucleophilic addition  
565 of nitrate, followed by radical fragmentation to yield the olefinic product. An equivalent of the  
566 nitrite radical is also generated, which oxidizes the host to reform the nitrate anion. This  
567 methodology was applied to achieve selective demethylenation in a dicyclopropanated steroid,  
568 providing exclusive generation of the double bond adjacent to the enone (**Figure 7g**). To expand  
569 on previous results from Fujita and co-workers on the photo-oxidation of adamantane with host-  
570 **15**,<sup>103,104</sup> Dasgupta and co-workers utilized host-**15** in the photo-oxidation of benzyl C–H bonds  
571 through host-guest charge transfer.<sup>105</sup> The host pre-organizes the substrate with solvent water  
572 molecules to assist with proton-coupled electron transfer, generating a neutral benzylic radical.  
573 Under irradiation and pressurized oxygen gas, the generated radical is oxidized to benzaldehyde.  
574 The system accommodated a range of toluene derivatives to produce the corresponding  
575 benzaldehyde product with >94% yield.

576           While the examples above require stoichiometric quantities of host, Su and co-workers  
577 reported a catalytic photodimerization using host-**61**, which incorporates a RuL<sub>3</sub> photocatalyst into  
578 its ligand scaffold.<sup>106</sup> Under blue LED light, host-**61** catalysed dimerization of naphthol derivatives  
579 in the presence of oxygen, to yield the corresponding naphthoquinone products (**Figure 7h**). The  
580 constricted cavity of the host enforced 1,4-coupling instead of the typically favoured 1,1-coupling  
581 to yield BINOL products. When the reaction was run with enantioresolved host-**61**, moderate  
582 enantioselectivity was achieved (up to 58% ee), albeit with lower yields.

583           As shown by these studies, supramolecular hosts assist photochemical reactions in unique  
584 ways, by pre-organizing encapsulated substrates to accelerate reaction rate, imposing  
585 stereocontrol, improving product selectivity, and in some cases acting as photosensitizers as well.



586

## 587 Figure 7: Photochemical Reactions Aided by Supramolecular Hosts

588 **a)** Electrocyclization catalysed by  $\beta$ -CD, followed by Pd/C reduction, reported by Aitken and co-  
 589 workers. **b)** Left: platinum photosensitizer tethered to  $\gamma$ -cyclodextrin. Right: head-to-tail  
 590 anthracene dimerization catalysed by host-49. **c)** Left: rim-modified  $\beta$ -cyclodextrins hosts **51a/b**  
 591 Right: slipped anthracene dimerization catalysed by 2:2  $\beta$ -cyclodextrin:anthracene complexes. **d)**  
 592 Left: sulphide-linked  $\beta$ -cyclodextrin dimer synthesized by Yang and co-workers. Right: highly  
 593 enantioselective anthracene dimerization catalysed by host-54. **e)** Anthracene dimerization,  
 594 reported by Ramamurthy and co-workers, catalysed by host-4. **f)** 1,3-rearrangement catalysed by  
 595 host-1, and table highlighting the effect of longer chains on the efficiency of rearrangement. **g)**  
 596 Top: mechanism for demethylenation of cyclopropanes catalysed by host-15. Bottom: application  
 597 of cyclopropane demethylenation to a steroid. **h)** Left: photosensitizing host synthesized by Su and  
 598 co-workers. Right: naphthol 1,4-dimerization catalysed by host-61.

599

600

## 601 **Conclusion**

602           Throughout this review, we have presented advances made at the interface of  
603 supramolecular catalysis and a wide range of synthetically relevant fields, including organic,  
604 organometallic, and photochemistry. These examples highlight the ability of supramolecular hosts  
605 to function as mechanistic probes to deconvolute microenvironment catalysis, and as useful  
606 catalysts in challenging organic transformations. Taken together, they also reveal key subsequent  
607 directions in which this field can expand.

608           The shift from proof-of-concept type reactivity to synthetic application is one of the  
609 frontiers of supramolecular chemistry, particularly involving asymmetric catalysis and site-  
610 selective reactivity. While the development of enantioenriched coordination cages presents a new  
611 way of controlling the chiral environment around reactive intermediates and transition states,  
612 systematic optimization of the host scaffold remains a major challenge. Fundamental progress  
613 directed towards the rational design of chiral host assemblies, including post-assembly  
614 modification and templating strategies, is needed for structure activity relationship studies and  
615 further development of supramolecular asymmetric methods.<sup>107</sup>

616           Site-selective supramolecular catalysis is another impactful application that warrants  
617 further investigation. The ability of a supramolecular host to maintain high reactivity on a partially  
618 encapsulated substrate presents the opportunity to target increasingly complex molecules, as  
619 demonstrated in the site-selective hydrogenation reaction by Toste, Raymond, Bergman, and co-  
620 workers.<sup>93</sup> We expect to see further applications of this supramolecular strategy in late-stage  
621 natural product functionalization and modification of biomolecules such as peptides and proteins.

622           Although significant progress has been made in the synthetic application of organic and  
623 organometallic host-mediated reactions, supramolecular reaction development in photochemistry



624 and electrochemistry is still a work in progress. Photochemical host-mediated reactivity is largely  
625 limited to proof-of-concept transformations such as intramolecular rearrangements, dimerization  
626 reactions, and cycloadditions. Initial efforts toward asymmetric and site-selective photochemical  
627 reactivity promoted by photoactive hosts show promise for further application-based studies.  
628 Light-responsive shape-shifting hosts, such as those developed by Clever and co-workers, may  
629 also enable new modes of reactivity as photo-switchable supramolecular catalysts.<sup>108</sup> Host-  
630 mediated strategies in electrochemistry have not yet been extensively explored, particularly  
631 regarding electrochemically active hosts. Recent reports by Schalley and co-workers indicate the  
632 ability of a supramolecular host to alter the redox potential of ferrocene *via* thermodynamic  
633 stabilization of ferrocenium upon encapsulation.<sup>109</sup> Lusby and co-workers reported a similar  
634 phenomenon, in which encapsulated quinone guests experience a shift in redox potential.<sup>110</sup> These  
635 findings suggest the potential of supramolecular hosts to facilitate otherwise challenging  
636 electrochemical transformations through selective stabilization of the reduced/oxidized form of  
637 the guest.

638 Finally, the last half-decade has seen major advances in theoretical analyses of  
639 supramolecular systems and the reactions that they mediate.<sup>111–115</sup> These calculations have been a  
640 long-standing challenge due to the large number of atoms typically associated in a supramolecular  
641 system, as well as other parameters such as the number of explicit solvent molecules within the  
642 cage. Theoretical calculations can be a useful mechanistic and predictive tool, particularly in real-  
643 time collaboration with the corresponding experimental work, and we anticipate a closer  
644 interaction between theoretical and supramolecular chemists in the future.

645

646

647 **Acknowledgements**

648 This work was supported by the Director, Office of Science, Office of Basic Energy Sciences, and  
649 the Division of Chemical Sciences, Geosciences, and Bioscience of the U.S. Department of Energy  
650 at Lawrence Berkeley National Laboratory (Grant DE-AC02-05CH1123).

651 **Author contributions**

652 †M.M., S.M.B., and K.T.X. contributed equally. All authors were involved in surveying the  
653 literature and structuring and editing the manuscript.

654 **Competing interests**

655 The authors declare no competing interests.

656 **References:**

- 657 1. Punekar, N. S. *ENZYMES: Catalysis, Kinetics and Mechanisms* (Springer Singapore, 2018).
- 658 2. Wolfenden, R. Degrees of difficulty of water-consuming reactions in the absence of  
659 enzymes. *Chem. Rev.* **106**, 3379–3396 (2006).
- 660 3. Radzicka, A. & Wolfenden, R. A proficient enzyme. *Science* **267**, 90–93 (1995).
- 661 4. Nothling, M. D. *et al.* Synthetic Catalysts Inspired by Hydrolytic Enzymes. *ACS Catal.* **9**,  
662 168–187 (2019).
- 663 5. Meeuwissen, J. & Reek, J. N. H. Supramolecular catalysis beyond enzyme mimics. *Nat.*  
664 *Chem.* **2**, 615–621 (2010).
- 665 6. Raynal, M., Ballester, P., Vidal-Ferran, A. & Van Leeuwen, P. W. N. M. Supramolecular  
666 catalysis. Part 2: Artificial enzyme mimics. *Chem. Soc. Rev.* **43**, 1734–1787 (2014).
- 667 7. Pedersen, C. J. Cyclic Polyethers and their Complexes with Metal Salts. *J. Am. Chem. Soc.*  
668 **89**, 2495–2496 (1967).
- 669 8. Lehn, J. M. Cryptates: The Chemistry of Macropolycyclic Inclusion Complexes. *Acc.*  
670 *Chem. Res.* **11**, 49–57 (1978).
- 671 9. Sherman, J. C. & Cram, D. J. Carcerand Interiors Provide a New Phase of Matter. *J. Am.*  
672 *Chem. Soc.* **111**, 4527–4528 (1989).
- 673 10. Cram, D. J. The Design of Molecular Hosts, Guests, and Their Complexes (Nobel Lecture).  
674 *Angew. Chem. Int. Ed.* **27**, 1009–1020 (1988).
- 675 11. Masson, E., Ling, X., Joseph, R., Kyeremeh-Mensah, L. & Lu, X. Cucurbituril chemistry:  
676 A tale of supramolecular success. *RSC Advances* **2**, 1213–1247 (2012).

- 677 12. Breslow, R. & Dong, S. D. Biomimetic reactions catalyzed by cyclodextrins and their  
678 derivatives. *Chem. Rev.* **98**, 1997–2011 (1998).
- 679 13. Barrow, S. J., Kasera, S., Rowland, M. J., Del Barrio, J. & Scherman, O. A. Cucurbituril-  
680 Based Molecular Recognition. *Chem. Rev.* **115**, 12320–12406 (2015).
- 681 14. Crini, G. Review: A history of cyclodextrins. *Chem. Rev.* **114**, 10940–10975 (2014).
- 682 15. Jon, S. Y., Ko, Y. H., Park, S. H., Kim, H. J. & Kim, K. A facile, stereoselective [2 + 2]  
683 photoreaction mediated by cucurbit[8]uril. *Chem. Commun.* **1**, 1938–1939 (2001).
- 684 16. Pattabiraman, M., Sivaguru, J. & Ramamurthy, V. Cucurbiturils as Reaction Containers for  
685 Photocycloaddition of Olefins. *Isr. J. Chem.* **58**, 264–275 (2018).
- 686 17. Zhang, Q. & Tiefenbacher, K. Hexameric resorcinarene capsule is a brønsted acid:  
687 Investigation and application to synthesis and catalysis. *J. Am. Chem. Soc.* **135**, 16213–  
688 16219 (2013).
- 689 18. Gibb, C. L. D. & Gibb, B. C. Well-defined, organic nanoenvironments in water: The  
690 hydrophobic effect drives a capsular assembly. *J. Am. Chem. Soc.* **126**, 11408–11409  
691 (2004).
- 692 19. Shimizu, K. D. & Rebek, J. Synthesis and assembly of self-complementary calix[4]arenes.  
693 *Proc. Natl. Acad. Sci. U. S. A.* **92**, 12403–12407 (1995).
- 694 20. Santamaría, J., Martín, T., Hilmersson, G., Craig, S. L. & Rebek, J. Guest exchange in an  
695 encapsulation complex: A supramolecular substitution reaction. *Proc. Natl. Acad. Sci. U. S.*  
696 *A.* **96**, 8344–8347 (1999).
- 697 21. Yoshizawa, M., Klosterman, J. K. & Fujita, M. Functional Molecular Flasks: New  
698 Properties and Reactions within Discrete, Self-Assembled Hosts. *Angew. Chem. Int. Ed.* **48**,  
699 3418–3438 (2009).
- 700 22. Mal, P., Schultz, D., Beyeh, K., Rissanen, K. & Nitschke, J. R. An Unlockable-Relockable  
701 Iron Cage by Subcomponent Self-Assembly. *Angew. Chem. Int. Ed.* **47**, 8297–8301 (2008).
- 702 23. Grommet, A. B., Feller, M. & Klajn, R. Chemical reactivity under nanoconfinement. *Nat.*  
703 *Nano.* **15**, 256–271 (2020).
- 704 24. Brown, C. J., Toste, F. D., Bergman, R. G. & Raymond, K. N. Supramolecular Catalysis in  
705 Metal–Ligand Cluster Hosts. *Chem. Rev.* **115**, 3012–3035 (2015).
- 706 25. Yoshizawa, M., Klosterman, J. K. & Fujita, M. Functional Molecular Flasks: New  
707 Properties and Reactions within Discrete, Self-Assembled Hosts. *Angew. Chemie Int. Ed.*  
708 **48**, 3418–3438 (2009).26. Fang, Y. *et al.* Catalytic reactions within the cavity of  
709 coordination cages. *Chemical Society Reviews* **48**, 4707–4730 (2019).
- 710 27. Catti, L., Zhang, Q. & Tiefenbacher, K. Advantages of Catalysis in Self-Assembled  
711 Molecular Capsules. *Chem. - A Eur. J.* **22**, 9060–9066 (2016).
- 712 28. Leenders, S. H. A. M., Gramage-Doria, R., De Bruin, B. & Reek, J. N. H. Transition metal  
713 catalysis in confined spaces. *Chemical Society Reviews* **44**, 433–448 (2015).

- 714 29. Dydio, P. & Reek, J. N. H. Supramolecular control of selectivity in transition-metal catalysis  
715 through substrate preorganization. *Chem. Sci.* **5**, 2135–2145 (2014).
- 716 30. Ramasamy, B. & Ghosh, P. The Developing Concept of Bifunctional Catalysis with  
717 Transition Metal N-Heterocyclic Carbene Complexes. *Eur. J. Inorg. Chem.* **2016**, 1448–  
718 1465 (2016).
- 719 31. Carboni, S., Gennari, C., Pignataro, L. & Piarulli, U. Supramolecular ligand-ligand and  
720 ligand-substrate interactions for highly selective transition metal catalysis. *Dalt. Trans.* **40**,  
721 4355–4373 (2011).
- 722 32. Pluth, M. D., Bergman, R. G. & Raymond, K. N. Acid catalysis in basic solution: A  
723 supramolecular host promotes orthoformate hydrolysis. *Science* **316**, 85–88 (2007).
- 724 33. Vy M. Dong, Dorothea Fiedler, Barbara Carl, Bergman, R. G. & Raymond, K. N. Molecular  
725 Recognition and Stabilization of Iminium Ions in Water. *J. Am. Chem. Soc.* **128**, 14464–  
726 14465 (2006).
- 727 34. Kaphan, D. M., Toste, F. D., Bergman, R. G. & Raymond, K. N. Enabling New Modes of  
728 Reactivity via Constrictive Binding in a Supramolecular-Assembly-Catalyzed Aza-Prins  
729 Cyclization. *J. Am. Chem. Soc.* **137**, 9202–9205 (2015).
- 730 35. Bierschenk, S. M., Bergman, R. G., Raymond, K. N. & Toste, F. D. A Nanovessel-  
731 Catalyzed Three-Component Aza-Darzens Reaction. *J. Am. Chem. Soc.* **142**, 733–737  
732 (2020).
- 733 36. Bräuer, T. M., Zhang, Q. & Tiefenbacher, K. Iminium Catalysis inside a Self-Assembled  
734 Supramolecular Capsule: Modulation of Enantiomeric Excess. *Angew. Chem. Int. Ed.* **55**,  
735 7698–7701 (2016).
- 736 37. Bräuer, T. M., Zhang, Q. & Tiefenbacher, K. Iminium Catalysis inside a Self-Assembled  
737 Supramolecular Capsule: Scope and Mechanistic Studies. *J. Am. Chem. Soc.* **139**, 17500–  
738 17507 (2017).
- 739 38. Catti, L. & Tiefenbacher, K. Intramolecular hydroalkoxylation catalyzed inside a self-  
740 assembled cavity of an enzyme-like host structure. *Chem. Commun.* **51**, 892–894 (2015).
- 741 39. Catti, L., Pöthig, A. & Tiefenbacher, K. Host-Catalyzed Cyclodehydration-Rearrangement  
742 Cascade Reaction of Unsaturated Tertiary Alcohols. *Adv. Synth. Catal.* **359**, 1331–1338  
743 (2017).
- 744 40. La Sorella, G., Sporni, L., Ballester, P., Strukul, G. & Scarso, A. Hydration of aromatic  
745 alkynes catalyzed by a self-assembled hexameric organic capsule. *Catal. Sci. Technol.* **6**,  
746 6031–6036 (2016).
- 747 41. Catti, L. & Tiefenbacher, K. Brønsted Acid-Catalyzed Carbonyl-Olefin Metathesis inside a  
748 Self-Assembled Supramolecular Host. *Angew. Chem. Int. Ed.* **57**, 14589–14592 (2018).
- 749 42. Christianson, D. W. Structural biology and chemistry of the terpenoid cyclases. *Chem. Rev.*  
750 **106**, 3412–3442 (2006).
- 751 43. Pronin, S. V. & Shenvi, R. A. Synthesis of highly strained terpenes by non-stop tail-to-head

- 752 polycyclization. *Nat. Chem.* **4**, 915–920 (2012).
- 753 44. Zhang, Q. & Tiefenbacher, K. Terpene cyclization catalysed inside a self-assembled cavity.  
754 *Nat. Chem.* **7**, 197–202 (2015).
- 755 45. Zhang, Q., Catti, L., Pleiss, J. & Tiefenbacher, K. Terpene Cyclizations inside a  
756 Supramolecular Catalyst: Leaving-Group-Controlled Product Selectivity and Mechanistic  
757 Studies. *J. Am. Chem. Soc.* **139**, 11482–11492 (2017).
- 758 46. Zhang, Q., Rinkel, J., Goldfuss, B., Dickschat, J. S. & Tiefenbacher, K. Sesquiterpene  
759 cyclizations catalysed inside the resorcinarene capsule and application in the short synthesis  
760 of isolongifolene and isolongifolenone. *Nat. Catal.* **1**, 609–615 (2018).
- 761 47. Zhang, Q. & Tiefenbacher, K. Sesquiterpene Cyclizations inside the Hexameric  
762 Resorcinarene Capsule: Total Synthesis of  $\delta$ -Selinene and Mechanistic Studies. *Angew.*  
763 *Chem. Int. Ed.* **58**, 12688–12695 (2019).
- 764 48. Syntrivanis, L. D. *et al.* Four-Step Access to the Sesquiterpene Natural Product  
765 Presilphiperfolan-1 $\beta$ -ol and Unnatural Derivatives via Supramolecular Catalysis. *J. Am.*  
766 *Chem. Soc.* **142**, 5894–5900 (2020).
- 767 49. Hong, C. M. *et al.* Deconvoluting the Role of Charge in a Supramolecular Catalyst. *J. Am.*  
768 *Chem. Soc.* **140**, 6591–6595 (2018).
- 769 50. Wang, K. *et al.* Electrostatic Control of Macrocyclization Reactions within Nanospaces. *J.*  
770 *Am. Chem. Soc.* **141**, 6740–6747 (2019).
- 771 51. Cullen, W., Misuraca, M. C., Hunter, C. A., Williams, N. H. & Ward, M. D. Highly efficient  
772 catalysis of the Kemp elimination in the cavity of a cubic coordination cage. *Nat. Chem.* **8**,  
773 231–236 (2016).
- 774 52. Cullen, W. *et al.* Catalysis in a Cationic Coordination Cage Using a Cavity-Bound Guest  
775 and Surface-Bound Anions: Inhibition, Activation, and Autocatalysis. *J. Am. Chem. Soc.*  
776 **140**, 2821–2828 (2018).
- 777 53. Holloway, L. R. *et al.* Tandem Reactivity of a Self-Assembled Cage Catalyst with  
778 Endohedral Acid Groups. *J. Am. Chem. Soc.* **140**, 8078–8081 (2018).
- 779 54. Howlader, P., Das, P., Zangrando, E. & Mukherjee, P. S. Urea-Functionalized Self-  
780 Assembled Molecular Prism for Heterogeneous Catalysis in Water. *J. Am. Chem. Soc.* **138**,  
781 1668–1676 (2016).
- 782 55. Martí-Centelles, V., Lawrence, A. L. & Lusby, P. J. High Activity and Efficient Turnover  
783 by a Simple, Self-Assembled ‘artificial Diels-Alderase’. *J. Am. Chem. Soc.* **140**, 2862–2868  
784 (2018).
- 785 56. Ueda, Y., Ito, H., Fujita, D. & Fujita, M. Permeable Self-Assembled Molecular Containers  
786 for Catalyst Isolation Enabling Two-Step Cascade Reactions. *J. Am. Chem. Soc.* **139**, 6090–  
787 6093 (2017).
- 788 57. Takezawa, H., Shitozawa, K. & Fujita, M. Enhanced reactivity of twisted amides inside a  
789 molecular cage. *Nat. Chem.* 1–5 (2020).

- 790 58. Hong, C. M., Bergman, R. G., Raymond, K. N. & Toste, F. D. Self-Assembled Tetrahedral  
791 Hosts as Supramolecular Catalysts. *Acc. Chem. Res.* **51**, 2447–2455 (2018).
- 792 59. Kaphan, D. M., Levin, M. D., Bergman, R. G., Raymond, K. N. & Toste, F. D. A  
793 supramolecular microenvironment strategy for transition metal catalysis. *Science* **350**,  
794 1235–1238 (2015).
- 795 60. Welborn, V. V., Li, W.-L. & Head-Gordon, T. Interplay of Water and a Supramolecular  
796 Capsule for Catalysis of Reductive Elimination Reaction from Gold. *Nat. Commun.* **11**, 415  
797 (2020).
- 798 61. Levin, M. D. *et al.* Scope and Mechanism of Cooperativity at the Intersection of  
799 Organometallic and Supramolecular Catalysis. *J. Am. Chem. Soc.* **138**, 9682–9693 (2016).
- 800 62. Bender, T. A., Morimoto, M., Bergman, R. G., Raymond, K. N. & Toste, F. D.  
801 Supramolecular Host-Selective Activation of Iodoarenes by Encapsulated Organometallics.  
802 *J. Am. Chem. Soc.* **141**, 1701–1706 (2019).
- 803 63. García-Simón, C. *et al.* Enantioselective hydroformylation by a Rh-catalyst entrapped in a  
804 supramolecular metallocage. *J. Am. Chem. Soc.* **137**, 2680–2687 (2015).
- 805 64. Jiao, J. *et al.* Design and Assembly of Chiral Coordination Cages for Asymmetric  
806 Sequential Reactions. *J. Am. Chem. Soc.* **140**, 2251–2259 (2018).
- 807 65. Yu, F. *et al.* Control over Electrochemical Water Oxidation Catalysis by Preorganization of  
808 Molecular Ruthenium Catalysts in Self-Assembled Nanospheres. *Angew. Chem. Int. Ed.* **57**,  
809 11247–11251 (2018).
- 810 66. Gonell, S., Caumes, X., Orth, N., Ivanović-Burmazović, I. & Reek, J. N. H. Self-assembled  
811 M12L24 nanospheres as a reaction vessel to facilitate a dinuclear Cu(i) catalyzed  
812 cyclization reaction. *Chem. Sci.* **10**, 1316–1321 (2019).
- 813 67. Wang, Q. *et al.* Self-assembled nanospheres with multiple endohedral binding sites pre-  
814 organize catalysts and substrates for highly efficient reactions. *Nat. Chem.* **8**, 225–230  
815 (2016).
- 816 678. Gonell, S. & Reek, J. N. H. Gold-catalyzed cycloisomerization reactions within  
817 guanidinium M12L24 nanospheres: the effect of local concentrations. *ChemCatChem* **11**,  
818 1458–1464 (2019).
- 819 69. Wang, S. *et al.* Ultrafine Pt Nanoclusters Confined in a Calixarene-Based {Ni<sub>24</sub>}  
820 Coordination Cage for High-Efficient Hydrogen Evolution Reaction. *J. Am. Chem. Soc.*  
821 **138**, 16236–16239 (2016).
- 822 70. Fang, Y. *et al.* Formation of a Highly Reactive Cobalt Nanocluster Crystal within a Highly  
823 Negatively Charged Porous Coordination Cage. *Angew. Chem. Int. Ed.* **57**, 5283–5287  
824 (2018).
- 825 71. Fang, Y. *et al.* Ultra-Small Face-Centered-Cubic Ru Nanoparticles Confined within a  
826 Porous Coordination Cage for Dehydrogenation. *Chem* **4**, 555–563 (2018).
- 827 72. Mondal, B., Acharyya, K., Howlader, P. & Mukherjee, P. S. Molecular Cage Impregnated

- 828 Palladium Nanoparticles: Efficient, Additive-Free Heterogeneous Catalysts for Cyanation  
829 of Aryl Halides. *J. Am. Chem. Soc.* **138**, 1709–1716 (2016).
- 830 73. Mondal, B. & Mukherjee, P. S. Cage Encapsulated Gold Nanoparticles as Heterogeneous  
831 Photocatalyst for Facile and Selective Reduction of Nitroarenes to Azo Compounds. *J. Am.*  
832 *Chem. Soc.* **140**, 12592–12601 (2018).
- 833 74. Yu, Y. & Rebek, J. Reactions of Folded Molecules in Water. *Acc. Chem. Res.* **51**, 3031–  
834 3040 (2018).
- 835 75. Mosca, S., Yu, Y., Gavette, J. V., Zhang, K. Da & Rebek, J. A Deep Cavitand Templates  
836 Lactam Formation in Water. *J. Am. Chem. Soc.* **137**, 14582–14585 (2015).
- 837 76. Wu, N., Petsalakis, I. D., Theodorakopoulos, G., Yu, Y. & Rebek, J. Cavitands as  
838 Containers for  $\alpha,\omega$ -Dienes and Chaperones for Olefin Metathesis. *Angew. Chem. Int. Ed.*  
839 **57**, 15091–15095 (2018).
- 840 77. Masseroni, D., Mosca, S., Mower, M. P., Blackmond, D. G. & Rebek, J. Cavitands as  
841 Reaction Vessels and Blocking Groups for Selective Reactions in Water. *Angew. Chem. Int.*  
842 *Ed.* **55**, 8290–8293 (2016).
- 843 78. Angamuthu, V., Rahman, F., Petroselli, M., Li, Y., Yu, Y. & Rebek, J. Mono epoxidation  
844 of  $\alpha,\omega$ -dienes using NBS in a water-soluble cavitand. *Org. Chem. Front.* **6**, 3220–3223  
845 (2019).
- 846 79. Angamuthu, V., Petroselli, M., Rahman, F. U., Yu, Y. & Rebek, J. Binding orientation and  
847 reactivity of alkyl  $\alpha,\omega$ -dibromides in water-soluble cavitands. *Org. Biomol. Chem.* **17**,  
848 5279–5282 (2019).
- 849 80. Shi, Q., Masseroni, D. & Rebek, J. Macrocyclization of Folded Diamines in Cavitands. *J.*  
850 *Am. Chem. Soc.* **138**, 10846–10848 (2016).
- 851 81. Takezawa, H., Kanda, T., Nanjo, H. & Fujita, M. Site-Selective Functionalization of Linear  
852 Diterpenoids through U-Shaped Folding in a Confined Artificial Cavity. *J. Am. Chem. Soc.*  
853 **141**, 5112–5115 (2019).
- 854 82. Fuertes-Espinosa, C. *et al.* Supramolecular Fullerene Sponges as Catalytic Masks for  
855 Regioselective Functionalization of C60. *Chem* **6**, 169–186 (2020).
- 856 83. García-Simón, C. *et al.* Sponge-like molecular cage for purification of fullerenes. *Nat.*  
857 *Commun.* **5**, 1–9 (2014).
- 858 84. Slagt, V. F., Reek, J. N. H., Kamer, P. C. J. & Leeuwen, P. W. N. M. van. Assembly of  
859 Encapsulated Transition Metal Catalysts. *Angew. Chem. Int. Ed.* **40**, 4271–4274 (2001).
- 860 85. Nurttala, S. S., Linnebank, P. R., Krachko, T. & Reek, J. N. H. Supramolecular approaches  
861 to control activity and selectivity in hydroformylation catalysis. *ACS Catal.* **8**, 3469–3488  
862 (2018).
- 863 86. Wang, X. *et al.* Tuning the Porphyrin Building Block in Self-Assembled Cages for  
864 Branched-Selective Hydroformylation of Propene. *Chem. Eur. J.* **23**, 14769–14777 (2017).
- 865 87. Nurttala, S. S. *et al.* Size-Selective Hydroformylation by a Rhodium Catalyst Confined in a

- 866 Supramolecular Cage. *Chem. Eur. J.* **25**, 609–620 (2018).
- 867 88. Bai, S. *et al.* Rational Redesign of a Regioselective Hydroformylation Catalyst for 3-  
868 Butenoic Acid by Supramolecular Substrate Orientation. *ChemCatChem* **11**, 5322–5329  
869 (2019).
- 870 89. Jongkind, L. J., Elemans, J. A. A. W. & Reek, J. N. H. Cofactor Controlled Encapsulation  
871 of a Rhodium Hydroformylation Catalyst. *Angew. Chem. Int. Ed.* **58**, 2696–2699 (2019).
- 872 90. Roland, S., Suarez, J. M. & Sollogoub, M. Confinement of Metal-N-Heterocyclic Carbene  
873 Complexes to Control Reactivity in Catalytic Reactions. *Chem. Eur. J.* **24**, 12464–12473  
874 (2018).
- 875 91. Zhang, P. *et al.* Cyclodextrin Cavity-Induced Mechanistic Switch in Copper-Catalyzed  
876 Hydroboration. *Angew. Chem. Int. Ed.* **56**, 10821–10825 (2017).
- 877 92. Xu, G. *et al.* Capturing the Monomeric (L)CuH in NHC-Capped Cyclodextrin: Cavity-  
878 Controlled Chemoselective Hydrosilylation of  $\alpha,\beta$ -Unsaturated Ketones. *Angew. Chem. Int.*  
879 *Ed.* **59**, 7591–7597 (2020)
- 880 93. Bender, T. A., Bergman, R. G., Raymond, K. N. & Toste, F. D. A Supramolecular Strategy  
881 for Selective Catalytic Hydrogenation Independent of Remote Chain Length. *J. Am. Chem.*  
882 *Soc.* **141**, 11806–11810 (2019).
- 883 94. Cram, D. J., Tanner, M. E. & Thomas, R. The Taming of Cyclobutadiene. *Angew. Chem.*  
884 *Int. Ed.* **30**, 1024–1027 (1991).
- 885 95. Mansour, A. T. *et al.*  $\beta$ -Cyclodextrin-Mediated Enantioselective Photochemical  
886 Electrocyclization of 1,3-Dihydro-2H-azepin-2-one. *J. Org. Chem.* **82**, 9832–9836 (2017).
- 887 96. Nakamura, A. & Inoue, Y. Supramolecular catalysis of the enantiodifferentiating [4 + 4]  
888 photocyclodimerization of 2-anthracenecarboxylate by  $\gamma$ -cyclodextrin. *J. Am. Chem. Soc.*  
889 **125**, 966–972 (2003).
- 890 97. Rao, M. *et al.* Photocatalytic Supramolecular Enantiodifferentiating Dimerization of 2-  
891 Anthracenecarboxylic Acid through Triplet-Triplet Annihilation. *Org. Lett.* **20**, 1680–1683  
892 (2018).
- 893 98. Wei, X. *et al.* Supramolecular Photochirogenesis Driven by Higher-Order Complexation:  
894 Enantiodifferentiating Photocyclodimerization of 2-Anthracenecarboxylate to Slipped  
895 Cyclodimers via a 2:2 Complex with  $\beta$ -Cyclodextrin. *J. Am. Chem. Soc.* **140**, 3959–3974  
896 (2018).
- 897 99. Ji, J. *et al.* An Ultimate Stereocontrol in Supramolecular Photochirogenesis:  
898 Photocyclodimerization of 2-Anthracenecarboxylate Mediated by Sulfur-Linked  $\beta$ -  
899 Cyclodextrin Dimers. *J. Am. Chem. Soc.* **141**, 9225–9238 (2019).
- 900 100. Wei, X. *et al.* Reversal of Regioselectivity during Photodimerization of 2-  
901 Anthracenecarboxylic Acid in a Water-Soluble Organic Cavitand. *Org. Lett.* **21**, 7868–7872  
902 (2019).
- 903 101. Dalton, D. M. *et al.* Supramolecular Ga<sub>4</sub>L<sub>6</sub> 12- cage photosensitizes 1,3-rearrangement of



- 904 encapsulated guest via photoinduced electron transfer. *J. Am. Chem. Soc.* **137**, 10128–10131  
905 (2015).
- 906 102. Cullen, W., Takezawa, H. & Fujita, M. Demethylenation of Cyclopropanes via  
907 Photoinduced Guest-to-Host Electron Transfer in an M6L4 Cage. *Angew. Chem. Int. Ed.*  
908 **58**, 9171–9173 (2019).
- 909 103. Yoshizawa, M., Miyagi, S., Kawano, M., Ishiguro, K. & Fujita, M. Alkane Oxidation via  
910 Photochemical Excitation of a Self-Assembled Molecular Cage. *J. Am. Chem. Soc.* **126**,  
911 9172–9173 (2004).
- 912 104. Furutani, Y. *et al.* In situ spectroscopic, electrochemical, and theoretical studies of the  
913 photoinduced host-guest electron transfer that precedes unusual host-mediated alkane  
914 photooxidation. *J. Am. Chem. Soc.* **131**, 4764–4768 (2009).
- 915 105. Das, A., Mandal, I., Venkatramani, R. & Dasgupta, J. Ultrafast photoactivation of CH bonds  
916 inside water-soluble nanocages. *Sci. Adv.* **5**, eaav4806 (2019).
- 917 106. Guo, J. *et al.* Regio- and Enantioselective Photodimerization within the Confined Space of  
918 a Homochiral Ruthenium/Palladium Heterometallic Coordination Cage. *Angew. Chem. Int.*  
919 *Ed.* **56**, 3852–3856 (2017).
- 920 107. Jongkind, L. J., Caumes, X., Hartendorp, A. P. T. & Reek, J. N. H. Ligand Template  
921 Strategies for Catalyst Encapsulation. *Acc. Chem. Res.* **51**, 2115–2128 (2018).
- 922 108. Li, R. J., Holstein, J. J., Hiller, W. G., Andréasson, J. & Clever, G. H. Mechanistic Interplay  
923 between Light Switching and Guest Binding in Photochromic [Pd2Dithienylethene4]  
924 Coordination Cages. *J. Am. Chem. Soc.* **141**, 2097–2103 (2019).
- 925 109. Jia, F. *et al.* Redox-Responsive Host-Guest Chemistry of a Flexible Cage with Naphthalene  
926 Walls. *J. Am. Chem. Soc.* **142**, 3306–3310 (2020).
- 927 110. Spicer, R. L. *et al.* Host-Guest-Induced Electron Transfer Triggers Radical-Cation  
928 Catalysis. *J. Am. Chem. Soc.* **142**, 2134–2139 (2020).
- 929 111. Vaissier Welborn, V. & Head-Gordon, T. Electrostatics Generated by a Supramolecular  
930 Capsule Stabilizes the Transition State for Carbon-Carbon Reductive Elimination from  
931 Gold(III) Complex. *J. Phys. Chem. Lett.* **9**, 3814–3818 (2018).
- 932 112. Ujaque, G., Maréchal, J. D. & Norjmaa, G. Reaction Rate Inside the Cavity of [Ga4L6]12-  
933 Supramolecular Metallo cage is Regulated by the Encapsulated Solvent. *Chem. Eur. J.* **26**,  
934 1–6 (2020).
- 935 113. Norjmaa, G., Maréchal, J. D. & Ujaque, G. Microsolvation and Encapsulation Effects on  
936 Supramolecular Catalysis: C-C Reductive Elimination inside [Ga4L6]12- Metallo cage. *J.*  
937 *Am. Chem. Soc.* **141**, 13114–13123 (2019).
- 938 114. Young, T. A., Martí-Centelles, V., Wang, J., Lusby, P. J. & Duarte, F. Rationalizing the  
939 Activity of an ‘artificial Diels-Alderase’: Establishing Efficient and Accurate Protocols for  
940 Calculating Supramolecular Catalysis. *J. Am. Chem. Soc.* **142**, 1300–1310 (2020).
- 941 115. Petroselli, M. *et al.* Radical Reactions in Cavitands Unveil the Effects of Affinity on

942 Dynamic Supramolecular Systems. *J. Am. Chem. Soc.* **142**, 2396–2403 (2020).

943